

UNCLASSIFIED

AD 404 519

*Reproduced
by the*

DEFENSE DOCUMENTATION CENTER

FOR

SCIENTIFIC AND TECHNICAL INFORMATION

CAMERON STATION, ALEXANDRIA, VIRGINIA



UNCLASSIFIED

NOTICE: When government or other drawings, specifications or other data are used for any purpose other than in connection with a definitely related government procurement operation, the U. S. Government thereby incurs no responsibility, nor any obligation whatsoever; and the fact that the Government may have formulated, furnished, or in any way supplied the said drawings, specifications, or other data is not to be regarded by implication or otherwise as in any manner licensing the holder or any other person or corporation, or conveying any rights or permission to manufacture, use or sell any patented invention that may in any way be related thereto.

63-3-4

REPORT NO.
TDR-169(3240-11)TN

SSD-TDR-63-30

CATALOGED BY AS
AS AD NO.

404 519

404 519

Yielding and Flow of the Body Centered Cubic Metals at Low Temperatures

7 MARCH 1963

Prepared by HANS CONRAD
Materials Sciences Laboratory

Prepared for COMMANDER SPACE SYSTEMS DIVISION

UNITED STATES AIR FORCE

Inglewood, California

DDC
RECORDED
MAY 21 1963
JISIA A



LABORATORIES DIVISION • AEROSPACE CORPORATION
CONTRACT NO. AF 04(695)-16

SSD-TDR-63-30

Report No.
TDR-169(3240-11)TN-5

YIELDING AND FLOW OF THE BODY CENTERED CUBIC
METALS AT LOW TEMPERATURES

Prepared by
Hans Conrad
Materials Sciences Laboratory

AEROSPACE CORPORATION
El Segundo, California

Contract No. AF 04(695)-169

7 March 1963

Prepared for
COMMANDER SPACE SYSTEMS DIVISION
UNITED STATES AIR FORCE
Inglewood, California

SSD-TDR-63-30

Report No.
TDR-169(3240-11)TN-5

YIELDING AND FLOW OF THE BODY CENTERED CUBIC
METALS AT LOW TEMPERATURES

7 March 1963

Prepared

H. Conrad

Hans Conrad, Head
Physics Department

Approved

J. E. Hove

J. E. Hove, Director
Materials Sciences Laboratory

AEROSPACE CORPORATION
El Segundo, California

ABSTRACT

The available experimental data on the mechanical behavior of the body centered cubic (b.c.c.) transition metals at low temperatures ($< 0.25 T_m$) are reviewed and analyzed to establish the rate-controlling mechanism responsible for the strong temperature and the strain-rate dependence of the yield and flow stresses. The activation energy, H , activation volume, v^* , and frequency factor, ν , were determined as a function of the thermal component of the stress, τ^* . It was found that H_0 ($\tau^* = 1 \text{ kg/mm}^2$) $\approx 0.1 \mu b^3$, where μ is the shear modulus and b the Burgers vector; $v^* \approx 50 b^3$ at $\tau^* = 2 \text{ kg/mm}^2$, increasing rapidly to values in excess of $100 b^3$ at lower stresses and decreasing to $2-5 b^3$ at high stresses ($50-60 \text{ kg/mm}^2$); and $\nu = 10^6 - 10^{12} \text{ sec}^{-1}$, the higher values of ν generally being associated with the purer materials. H and v^* , as a function of stress, were independent of structure. This along with other observations indicates that the thermally-activated overcoming of the Peierls-Nabarro stress is the rate-controlling mechanism. The values of H_0 and the change in H with stress at low stresses are in agreement with those predicted by Seeger's model for the nucleation of kinks. The Peierls-Nabarro stress and kink energy derived from the experimental data are approximately $10^{-2} \mu$ and $4 \times 10^{-2} \mu b^3$, respectively.

The experimental data suggest that the yield point in the b.c.c. metals is associated with the sudden multiplication of dislocations by the double cross-slip mechanism, which in turn is controlled by the motion of dislocations through the lattice. Stress-strain curves for mild steel calculated on the basis of this mechanism are in good agreement with the experimental curves.

ACKNOWLEDGEMENT

The author wishes to express appreciation to B. L. Mordike, G. A. Sargent, P. J. Sherwood, A. A. Johnson, R. Chambers, J. W. Christian and B. C. Masters for submitting data previous to publication. He also wishes to acknowledge the valuable assistance of G. Stone for making calculations and plotting graphs.

CONTENTS

I.	INTRODUCTION	1
II.	EXPERIMENTAL DATA	3
	A. Effect of Temperature on Yield and Flow Stresses	3
	1. Microdeformation	3
	2. Macrodeformation	4
	B. Effect of Strain Rate on the Yield and Flow Stresses	7
	C. Activation Energy, Activation Volume, and Frequency Factor for Deformation	8
	1. General	8
	2. Activation Energy, H	10
	3. Activation Volume, v^*	11
	4. Frequency Factor, ν	11
III.	DISCUSSION	14
	A. Rate-Controlling Mechanism	14
	B. Yield Point and Work Hardening	23

TABLES

1.	Values of T_0 and the Ratio of T_0/T_m for Pure and Impure B. C. C. Metals	6
2.	Values of τ_0^* Obtained by Extrapolating τ^* to 0°K	7
3.	The Frequency Factor, ν , for the B. C. C. Metals Obtained from Yield or Flow Stress Measurements	12
4.	Values of ν Derived from the Effect of Strain Rate on the Ductile-to-Brittle Transition Temperature	13
5.	Evidence Against Specific Mechanisms Proposed as Rate-Controlling During the Low Temperature Deformation of the B. C. C. Metals	15
6.	Values of H_0 , H_K , and H_{PN} Derived from the Experimental Data	18
7.	Values of w and l^* Derived from the Experimental Data	19
8.	Effect of Strain on the Dislocation Density Participating in the Plastic Flow of Iron Determined from the Frequency Factor ν	21

FIGURES

1. Initial Yield Stress of Various Polycrystalline Metals vs Ratio of T/T_m
2. Effect of Strain Rate on the Yield and Flow Stresses of F. C. C. and B. C. C. Metals
3. Idealized Stress-Strain Curves for an Ultrapure Iron at Two Temperatures
4. Temperature Dependence of σ_A for Various Materials and State of Locking
5. Effect of Temperature on the Initial Yield Stress, the Proportional Limit After Straining, and the Flow Stress of Electrolytic Iron.
6. Effect of Temperature on the Thermal Component of the Yield Stress of Tungsten
7. Variation of τ^* with Temperature for Pure (<0.005 wt % Interstitials) and Impure (>0.02 wt % Interstitials) Group VA Metals, Strain Rate 10^{-4} sec^{-1}
8. Variation of τ^* with Temperature for Pure (<0.005 wt % Interstitials) and Impure (>0.02 wt % Interstitials) Group VIA Metals, Strain Rate 10^{-4} sec^{-1}
9. Variation of τ^* with Temperature for Pure (<0.005 wt % Interstitials) and Impure (>0.02 wt % Interstitials) Iron.
10. Temperature Dependence of Reversible Flow Stress in Iron.
11. Log τ^* vs Temperature for Impure Polycrystalline B. C. C. Metals
12. Effect of Stress on the Activation Energy for the Deformation of Vanadium
13. Effect of Stress on the Activation Energy for the Deformation of Niobium
14. Effect of Stress on the Activation Energy for the Deformation of Tantalum.

FIGURES

1. Initial Yield Stress of Various Polycrystalline Metals vs Ratio of T/T_m
2. Effect of Strain Rate on the Yield and Flow Stresses of F. C. C. and B. C. C. Metals
3. Idealized Stress-Strain Curves for an Ultrapure Iron at Two Temperatures
4. Temperature Dependence of σ_A for Various Materials and State of Locking
5. Effect of Temperature on the Initial Yield Stress, the Proportional Limit After Straining, and the Flow Stress of Electrolytic Iron.
6. Effect of Temperature on the Thermal Component of the Yield Stress of Tungsten
7. Variation of τ^* with Temperature for Pure (<0.005 wt % Interstitials) and Impure (>0.02 wt % Interstitials) Group VA Metals, Strain Rate 10^{-4} sec^{-1}
8. Variation of τ^* with Temperature for Pure (<0.005 wt % Interstitials) and Impure (>0.02 wt % Interstitials) Group VIA Metals, Strain Rate 10^{-4} sec^{-1}
9. Variation of τ^* with Temperature for Pure (<0.005 wt % Interstitials) and Impure (>0.02 wt % Interstitials) Iron.
10. Temperature Dependence of Reversible Flow Stress in Iron.
11. Log τ^* vs Temperature for Impure Polycrystalline B. C. C. Metals
12. Effect of Stress on the Activation Energy for the Deformation of Vanadium
13. Effect of Stress on the Activation Energy for the Deformation of Niobium
14. Effect of Stress on the Activation Energy for the Deformation of Tantalum.

FIGURES (Continued)

15. Effect of Stress on the Activation Energy for the Deformation of Chromium
16. Effect of Stress on the Activation Energy for the Deformation of Molybdenum.
17. Effect of Stress on the Activation Energy for the Deformation of Tungsten.
18. Effect of Stress on the Activation Energy for Yielding and Flow in Iron and Steel
19. Relationship Between H_0 ($\tau^* = 1 \text{ kg/mm}^2$) and μb^3 for the B. C. C. Metals
20. Activation Energy vs Log τ^* for the B. C. C. Metals
21. Effect of Stress on the Activation Volume for the Deformation of Tantalum.
22. Effect of Stress on the Activation Volume for the Deformation of Tungsten.
23. Effect of Stress on the Activation Volume for Yielding and Flow in Iron and Steel
24. Effect of Stress on the Activation Volume for Deformation of the B. C. C. Transition Metals.
25. Variation of Activation Energy with Temperature for Ingot Iron and Mild Steel
26. Variation of Activation Energy with Temperature for Impure Polycrystalline B. C. C. Metals.
27. Variation of the Activation Energy for Brittle Fracture with Temperature.
28. Seeger's Model for Thermally-Activated Overcoming of the Peierls-Nabarro Energy

FIGURES (Continued)

29. Variation of Activation Energy with Temperature for Electrolytic Iron, Water Quenched from 920°C
30. Variation of Activation Energy with Temperature for Ferrovac Iron
31. Comparison of Calculated and Experimental Stress-Strain Curves for Mild Steel

I. INTRODUCTION

A distinguishing feature of the body centered cubic (b. c. c.) metals, as compared to the close packed hexagonal (c. p. h.), and face centered cubic (f. c. c.) metals, is the strong effect of temperature and of strain rate on the yield stress at low temperatures ($T < 0.2 T_m$, where T is the test temperature and T_m is the melting temperature), Figs. 1 and 2. An understanding of this difference is of technological, as well as of scientific interest, because the ductile-to-brittle transition in the b. c. c. metals is related to the strong temperature and to the strong strain-rate dependence of the yield stress.

A number of thermally-activated dislocation mechanisms have been proposed to account for the strong temperature and for the strong strain-rate dependence of the yield stress of the b. c. c. metals. In chronological order, these are:

- a) breaking away from an interstitial atmosphere (Refs. 1-4)
- b) overcoming of the Peierls-Nabarro stress (Refs. 5-9)[†]
- c) nonconservative motion of jogs (Refs. 11-13)
- d) overcoming of the interstitial precipitates (Ref. 14)
- e) cross-slip (Ref. 15)

There is some experimental support for each of these mechanisms, which makes it difficult to decide which one is actually rate-controlling. From a review of the experimental data for iron available at the time, Conrad (Ref. 6) concluded that the best overall agreement was for the thermally-activated overcoming of the Peierls-Nabarro stress. Subsequent research

[†]Heslop and Petch (Ref. 10) first suggested that the strong temperature dependence of the yield and flow stress in iron might be due to a high Peierls-Nabarro stress. However, they attributed the temperature dependence to a change in width of the dislocation with temperature rather than the contribution of thermal fluctuations to overcoming of the Peierls-Nabarro stress. Their suggestion does not account for the strong effect of strain rate on the yield stress.

on iron (Refs. 8, 16) supported this conclusion. Recently, Conrad and Hayes (Ref. 9) analyzed the available data for the Group VA (V, Nb, Ta) and Group VIA (Cr, Mo, W) metals and again concluded that the rate-controlling mechanism at low temperatures was overcoming the Peierls-Nabarro stress. A similar conclusion was reached by Basinski and Christian (Ref. 5) for iron and by Christian and Masters (Ref. 7) for the Group VA metals.

In the present paper, pertinent data for all the b. c. c. transition metals are reviewed (including some of the more recent data, Refs. 7, 13, 17-19), and the rate-controlling mechanism during low temperature deformation is re-examined.

II. EXPERIMENTAL DATA

A. EFFECT OF TEMPERATURE ON YIELD AND FLOW STRESSES

1. Microdeformation

Employing a strain sensitivity of 4×10^{-6} and a strain rate of $\sim 10^{-3} \text{ sec}^{-1}$, Brown and Ekvall (Ref. 15) found that the stress-strain behavior of ultrapure ($\sim 0.004 \text{ wt } \%$ interstitials) and impure ($\sim 0.04 \text{ wt } \%$ interstitials) iron consisted of three distinct regions, Fig. 3.

σ_E^\dagger is the stress where a hysteresis loop is first observed upon loading and unloading and represents the first evidence of dislocation motion. σ_E was only observed after previous straining ($\epsilon = 10^{-4}$ to 5×10^{-2}).

σ_A is the stress at which a permanent strain first occurs, i. e., the lowest stress at which the hysteresis loop does not close. This is generally the same as the stress at which a deviation from linearity can be measured and is usually called the proportional limit.

σ_F is commonly called yield or flow stress.

Brown and Ekvall (Ref. 15) found that σ_E was independent of temperature (between 300° and 78°K) for the impure and pure irons. The variation of σ_A with temperature is shown in Fig. 4. σ_A for the locked state (undeformed impure iron) here exhibits about the same temperature dependence as that previously reported (Refs. 20, 21) for the lower yield stress (of annealed or strain-aged states) and the subsequent flow stress of various impure irons ($C + N > 0.015 \text{ wt } \%$) and steels. $\dagger\dagger$ On the other hand, σ_A for the unlocked (deformed) state has a lower temperature dependence than for yielding or for

\dagger Throughout the present paper σ will be used to designate tensile stress and τ shear stress. It will be assumed that $\tau = 1/2 \sigma$. Similarly, $\dot{\epsilon}$ is the tensile strain rate and $\dot{\gamma}$ the shear strain rate; $\dot{\gamma} = 0.7 \dot{\epsilon}$.

$\dagger\dagger$ Data on the other b. c. c. metals also indicate that the proportional limit of annealed impure ($> 0.02 \text{ wt } \%$ interstitials) material has a temperature dependence similar to that for the subsequent yield and flow stresses (Refs. 9, 20).

subsequent flow. Additional evidence that the proportional limit, σ_A , after prestraining has a weaker temperature dependence than the flow stress, σ_F , of iron has been reported by Conrad and Frederick (Ref. 8), Fig. 5, and by Kitajima (Ref. 22).

2. Macrodeformation

The yield or flow stress, τ , of b. c. c. metals can be considered to consist of three components (Refs. 6, 10, 20, 21):

$$\bullet \tau = \tau^*(T, \dot{\gamma}) + \tau_{\mu} + Kd^{-1/2} \quad (1)$$

τ^* is the thermal component which depends on temperature, T , and strain rate, $\dot{\gamma}$, and is associated with thermally-assisted overcoming of short-range obstacles. τ_{μ} represents the athermal component associated with long-range stress fields, is independent of strain rate, and varies with temperature only through the temperature variation of the shear modulus, μ . $Kd^{-1/2}$ is the component representing the grain size effect. K is the slope of the plot of the yield or flow stress versus the reciprocal of the square root of the grain size, d , and for annealed impure material it is relatively independent of temperature and strain rate when compared to τ^* (Refs. 21, 23-26). When K is independent of grain size, $Kd^{-1/2}$ gives the Hall-Petch relation (Refs. 27, 28). However, there are indications (Ref. 29) that K , for both the lower-yield stress and flow stress, is a function of the grain size, and therefore the effect of grain size is not given by the simple Hall-Petch equation.

In the present discussion, we are principally concerned with the effect of temperature on the thermal component, τ^* , and wish to separate it from the others. This is accomplished by subtracting the stress at a given

temperature, T , from that at some reference temperature T° (Refs. 6, 20), assuming that K is relatively independent of temperature, i. e.,

$$\tau_T - \tau_{T^{\circ}} = \tau^*(T, \dot{\gamma}) - \tau^*(T^{\circ}, \dot{\gamma}) = \Delta\tau^*(T, \dot{\gamma}) \quad (2)$$

Typical results on iron and tungsten are shown in Figs. 5 and 6. Similar plots have been developed previously for iron (Ref. 20) and the Group VA and VIA metals (Refs. 9, 20). τ^* as a function of temperature is then derived from such plots by taking $\tau^* = 0$ at the temperature T_0 , obtained by extrapolating plots of $\log(\partial\tau^*/\partial\tau)$ versus T to a value of $\sim 5 \times 10^{-3}$ $\text{kg}/(\text{mm}^2 - ^{\circ}\text{K})$, where $[(1/\tau)(d\tau/dT)] \approx [(1/\mu)(d\mu/dT)]$ and hence $\tau \approx \tau_{\mu}$. ($\partial\tau^*/\partial T$ is obtained by graphical differentiation of average curves similar to those in Figs. 5 and 6.) Plots of τ^* for yielding versus temperature for a strain rate of $\sim 10^{-4} \text{ sec}^{-1}$ derived in this manner from the available experimental data are given in Figs. 7-9. It is seen here that for the Group VA metals the variation of τ^* with temperature is relatively independent of purity and grain size (i. e., whether the specimen is single or polycrystalline), while for the Group VIA metals and iron, τ^* as a function of temperature is clearly dependent on purity and grain size. For the Group VIA metals and iron, the upper limit of τ^* at a given temperature is for polycrystals with interstitial contents $\geq 0.02 \text{ wt } \%$; the lower limit is for single crystals and polycrystals with less than $0.005 \text{ wt } \%$ interstitials. Single crystals and polycrystals with intermediate impurity levels exhibited a variation of τ^* with temperature between these two limits. In general, for the impure materials, τ^* at a given temperature was less for single crystals than for polycrystals of the same impurity content. Figures 5 and 10 show that previous thermal treatment and deformation may also influence the temperature dependence of τ^* .

Values of T_0 (to the nearest 50°K) for a strain rate of 10^{-4} sec^{-1} are given in Table 1. For the Group VIA metals and iron, T_0 for the pure materials is less than that for the impure materials, whereas for the Group V metals

there is no significant effect of impurity content on T_0 . This difference and the difference in the effect of impurity content on the temperature dependence of τ^* may be related to the higher solubility of interstitials in the Group VA metals compared to the Group VIA metals and iron.

Table 1. Values of T_0 and the Ratio of T_0/T_m for Pure and Impure B. C. C. Metals

Metal	$T_m, ^\circ K$	$T_0, ^\circ K$		T_0/T_m	
		Pure	Impure	Pure	Impure
V	2137	---	500	----	0.23
Nb	2741	500	500	0.18	0.18
Ta	3269	600	600	0.18	0.18
Cr	2148	---	500	----	0.26
Mo	2883	450	700	0.16	0.24
W	3683	500	850	0.14	0.23
Fe	1810	300	350	0.16	0.19

Pure b. c. c. metals (< 0.005 wt % interstitials)
 Impure b. c. c. metals (> 0.02 wt % interstitials)
 Strain rate 10^{-4} sec^{-1}

From Table 1 it is seen that the ratio T_0/T_m is 0.22 ± 0.04 for all impure polycrystalline b. c. c. metals. In a previous paper (Ref. 9) it was shown that the yield stresses of all the impure polycrystalline b. c. c. metals correlate rather well on a single curve when τ^* is plotted versus the parameter $(T - T_0)/T_m$.

Values of τ_0^* obtained by extrapolating the curves of Figs. 7-9 to $0^\circ K$ are given in Table 2. Because of the rapid increase in τ^* at very low temperatures, there is some uncertainty associated with these values. However, if one plots the logarithm of τ^* versus temperature, an approximately linear region occurs at low temperatures (Fig. 11) allowing for an easier extrapolation. Extrapolation of this linear region to $0^\circ K$ gives values of τ_0^*

slightly higher than those based on the linear plots, Table 2. Both methods yield values of τ_0^* of the order of $10^{-2}\mu$.

Table 2. Values of τ_0^* Obtained by Extrapolating τ^* to 0°K

Metal	μ $\times 10^3 \text{ kg/mm}^2$	τ_0^* , kg/mm^2				$\tau_0^*(\text{Avg})/\mu$ $\times 10^{-2}$
		τ^* vs T	$\log \tau^*$ vs T	H vs $\log \tau^*$	Avg	
V	5.2	60	65	60	62	1.19
Nb	4.0	58	65	60	61	1.52
Ta	7.0	60	67	80	69	0.99
Cr	11.4	79	90	80	83	0.73
Mo	12.7	78	105	85	89	0.70
W	15.7	100	165	100	122	0.78
Fe	7.4	49	65	60	58	0.78

$\mu = 3/8 E$, where E is Young's modulus at 300°K (Tietz and Wilson, Ref. 30).

B. EFFECT OF STRAIN RATE ON THE YIELD AND FLOW STRESSES

In Fig. 2 the typical variation of the strain-rate parameter, $\Delta\sigma/\Delta \ln \dot{\epsilon}$ ($\Delta\sigma$ is the incremental increase in yield or flow stress for an increase in strain rate from $\dot{\epsilon}_1$ to $\dot{\epsilon}_2$), with temperature for the b. c. c. metals is shown.† It initially increases with decrease in temperature below T_0 , goes through a maximum, and then decreases again, approaching zero as the temperature goes to absolute zero. It depends on structure (i. e., on impurities and on thermal and mechanical history) in a similar manner, as does the parameter $\Delta\tau^*/\Delta T$; e. g., compare the effect of strain on $\Delta\sigma/\Delta \ln \dot{\epsilon}$ and on $\Delta\tau^*/\Delta T$ for iron in Figs. 2 and 5.

† More detailed data on the variation of $\Delta\sigma/\Delta \ln \dot{\epsilon}$ with temperature are found in Refs. 5, 7, 8, and 13.

Another type of experiment which also gives the relationship between the yield stress and strain rate is the so-called delay-time test employed by Wood and Clark (Ref. 31) and Kraft and Sullivan (Ref. 32). In general, the parameter $\Delta\sigma/\Delta \ln t_d$, where t_d is the delay time for yielding, obtained from such tests has a similar value and exhibits the same trends as does the parameter $\Delta\sigma/\Delta \ln \dot{\epsilon}$.

C. ACTIVATION ENERGY, ACTIVATION VOLUME, AND FREQUENCY FACTOR FOR DEFORMATION

1. General

It is now generally accepted that the deformation of metals may be thermally activated, and if a single mechanism is rate-controlling one can write for the shear strain rate $\dot{\gamma}$

$$\dot{\gamma} = \rho b \dot{s} = \rho b s v^* \exp\left[-\frac{H(\tau, T)}{kT}\right] \quad (3)$$

where ρ is the density of dislocations contributing to the deformation, b the Burgers vector, \dot{s} the average velocity of the dislocations, s the product of the number of places where thermal activation can occur per unit length of dislocation and the area swept out per successful thermal fluctuation, v^* the frequency of vibration of the dislocation segment involved in the thermal activation, and H the activation enthalpy (energy) which may be a function of the shear stress, τ , and the temperature, T . For the b. c. c. metals, it has been established (Refs. 6, 8, 9, 16) that H is primarily a function of the effective shear stress, τ^* (i. e., the thermal component of the yield or flow stress) given by the difference between the applied stress, τ , and the long range internal stress τ_μ , i. e., $\tau^* = \tau - \tau_\mu$. Further, one can show that (Ref. 33)

$$H = -k \left(\frac{\partial \ln \dot{\gamma}/\nu}{\partial 1/T} \right)_{\tau^*} \quad (4a)$$

$$= -kT^2 \left(\frac{\partial \ln \dot{\gamma}/\nu}{\partial \tau} \right)_T \left(\frac{\partial \tau^*}{\partial T} \right)_{\dot{\gamma}} \quad (4b)$$

Rearranging Eq. 3 and differentiating

$$-\frac{dH}{d\tau^*} = kT \left(\frac{\partial \ln \dot{\gamma}/\nu}{\partial \tau} \right)_T \quad (5a)$$

$$= \frac{k \ln (\dot{\gamma}/\nu)}{(\partial \tau^*/\partial T)_{\dot{\gamma}}} \quad (5b)$$

where $\nu = \rho b s \nu^*$ and $-dH/d\tau^*$ is defined as the activation volume, ν^* . The value of ν can be obtained from the relations

$$H = kT \ln \left(\frac{\nu}{\dot{\gamma}} \right) \quad (6a)$$

or

$$-T \left(\frac{\partial \ln \dot{\gamma}}{\partial \tau} \right)_T \left(\frac{\partial \tau^*}{\partial T} \right) = \ln \left(\frac{\nu}{\dot{\gamma}} \right) \quad (6b)$$

i.e., from the slope of a plot of H versus T or a plot of $(\partial \tau^*/\partial T)_{\dot{\gamma}}$ versus $(1/T)(\partial \tau/\partial \ln \dot{\gamma})_T$. If ν is relatively independent of temperature and stress per se, the values of H , ν^* , and ν can then be derived from the relationships between stress, temperature, and strain rate obtained from the usual

mechanical tests.† For polycrystalline b. c. c. metals (and also single crystals), a reasonable assumption is that $\tau = 1/2 \sigma$, and $\gamma = 0.7 \epsilon$, where σ is the tensile stress, and ϵ is the tensile strain; also, $(\partial \tau^*/\partial T)_\gamma$ is approximated by $(\partial \tau/\partial T)_\gamma$, because $d\tau_\mu/\partial T$ is small compared to $(\partial \tau^*/\partial T)$.

2. Activation Energy, H

The variation of H with τ^* obtained from the available experimental data is shown in Figs. 12-18. Identical results were obtained from the use of either Eq. (4a) or (4b), supporting the validity of the assumptions inherent in these equations. The curves drawn in these figures represent the author's interpretation of the variation of H with τ^* indicated by the data points. However, there is some doubt as to whether a change in curvature actually occurs at the low stress, and for the most part the data suggest equally well a rather rapid increase in H as τ^* approaches zero. Of particular significance in Figs. 12-18 is that, within the scatter of the data, H as a function of τ^* is independent of the yielding or flow phenomena considered (microcreep, delay time, proportional limit, upper yield stress, flow, and dislocation velocity) and of the structure (impurity content, grain size, and previous thermal or mechanical history) for a given metal. In Fig. 19, it is seen that H_0 , the value of H at $\tau^* = 1 \text{ kg/mm}^2$, is approximately equal to $0.1 \mu b^3$, when comparing the various b. c. c. metals.††

A number of investigators (Refs. 2, 6, 34-36) have reported that the activation energy for yielding in iron decreases in a linear manner with the logarithm of the total applied stress, τ . For comparison, plots of H versus $\log \tau^*$ are given in Fig. 20 for the various impure polycrystalline

† The values of H, v^* , and the product sv^* can also be obtained from measurements of the effect of stress and temperature on dislocation velocity by replacing the strain rate, $\dot{\epsilon}$, in Eqs. 4-6 with the velocity, \dot{s} .

†† The shear modulus values were derived from the relation $\mu = 3/8 E$, where E is the Young's modulus at T_0 , (Ref. 30).

b. c. c. metals.† It is seen here that for such plots there appears to be two linear regions, one at very low stresses and the other at high stresses, with a transition region in the vicinity of $\tau^* = 1-5 \text{ kg/mm}^2$. The slope in the high stress region is about 10 times that in the low stress region. Extrapolation of the straight lines at high stresses to $H = 0$ gives values of τ_0^* in reasonable agreement with those obtained by the other two methods, Table 2.

3. Activation Volume, v^*

Typical variation of v^* with τ^* is shown for Ta, W, and Fe in Figs. 21-23. There was agreement between values obtained from Eq. (5a) and Eq. (5b) and from graphical differentiation of the curves of Figs. 12-18, except at the lowest values of τ^* .†† It is shown in Fig. 24 that the activation volume as a function of stress is similar for all the b. c. c. metals. The values given here were taken from average curves, such as those drawn in Figs. 21-23. It is seen from Fig. 24 that, for all of the b. c. c. metals, v^* is about $50 b^3$ at $\tau^* = 2 \text{ kg/mm}^2$, increasing rapidly to values in excess of $100 b^3$ at lower values of stress and decreasing with stress to values as low as $2-5 b^3$. Again, as for H, v^* as a function of stress is independent of the yielding or flow phenomena considered and of the structure, i. e., of mechanical and thermal history.

4. Frequency Factor, ν

Typical proportionality between H and temperature obtained for the b. c. c. metals is shown in Fig. 25. Plots of the average curves of H vs T for all the impure polycrystalline b. c. c. metals are given in Fig. 26. Average values of ν derived from such plots for pure ($< 0.005 \text{ wt } \%$) and impure ($> 0.02 \text{ wt } \%$) materials are given in Table 3.

† The values of H and τ^* plotted in Fig. 20 were taken from the average curves drawn in Figs. 12-18.

†† This disagreement will be discussed in a subsequent section.

Table 3. The Frequency Factor, ν , for the B. C. C. Metals
Obtained from Yield or Flow Stress Measurements

Metal	Authors	ν , sec ⁻¹	
		Pure Single or Polycrystals	Impure Polycrystals
V	Conrad, Present	---	10 ⁶
	Christian and Masters (Ref. 7)	---	10 ¹⁰
Nb	Conrad, Present	10 ⁶	10 ⁶
	Christian and Masters (Ref. 7)	---	10 ⁸
Ta	Conrad, Present	10 ⁸	10 ⁸
	Chambers (Ref. 39)	10 ⁷	---
	Christian and Masters (Ref. 7)	---	10 ¹¹
	Mordike (Ref. 13)	10 ⁹	---
Cr	Conrad, Present	---	10 ⁹
Mo	Conrad, Present	10 ¹¹	10 ⁶
W	Conrad, Present	10 ¹¹	10 ⁷
Fe	Conrad, Present	10 ¹¹	10 ⁸
	Basinski and Christian (Ref. 5)	---	10 ⁸
	Conrad (Ref. 6)	---	10 ⁸ - 10 ⁹
	Lean, Plateau, and Crussard (Ref. 38)	---	10 ⁸ - 10 ¹⁰

Additional evidence of the proportionality between H and temperature is provided by the variation of the ductile-to-brittle transition temperature in the b. c. c. metals with strain rate. Generally, a straight line is obtained when the logarithm of the strain rate is plotted versus the reciprocal of the transition temperature (Refs. 37, 38), suggesting a rate equation of the form $\dot{\epsilon} = Ae^{-H/kT}$. Taking the logarithm of both sides of this equation and rearranging, one obtains $H = kT \ln A/\dot{\epsilon}$ (Fig. 27), which

agrees with Eq. 6 when $A = \nu$. This is consistent with the analysis of Eqs. 3-6, if the transition from ductile-to-brittle behavior occurs at a constant stress. The values of ν derived from the effect of strain rate on the ductile-to-brittle transition are given in Table 4. They are in reasonable agreement with those obtained from the yield and flow stress measurements listed in Table 3, indicating that the ductile-to-brittle transition temperature is determined by the dynamic motion of dislocations, as has been proposed by Cottrell (Ref. 40) and Petch (Ref. 24).

Table 4. Values of ν Derived from the Effect of Strain Rate on the Ductile-to-Brittle Transition Temperature (Refs. 37 and 38)

Metal	ν, sec^{-1}
Cr	10^{10}
Mo	$10^8 - 10^{12}$
W	10^{12}
Fe	$10^8 - 10^{12}$

III. DISCUSSION

A. RATE-CONTROLLING MECHANISM

The fact that the various relationships of Eqs. 3-6 gave the same values of H , v^* , and v indicates that the postulated assumptions are valid, at least to a first approximation. Specifically, this supports the contention that during the low temperature deformation ($< 2.0 T_m$) of the b. c. c. transition metals, a single dislocation mechanism is rate-controlling and that v is relatively independent of stress and temperature per se. Furthermore, the fact that identical values of H and v^* were obtained for all yielding and flow phenomena (and the ductile-to-brittle transition) indicates that the same dislocation mechanism is controlling in all cases and that this is associated with the motion of dislocations through the lattice, as distinct from a generation mechanism, such as breaking away from an interstitial atmosphere. Finally, the fact that H and v^* as a function of stress were independent of structure (i. e. , thermal and mechanical history) strongly suggests that the rate-controlling mechanism is overcoming the inherent resistance of the lattice, i. e. , overcoming the Peierls-Nabarro stress. Further support for the Peierls-Nabarro mechanism is that dislocations in the b. c. c metals are often observed to lie along the close-packed directions (Ref. 41-43). A summary of the experimental evidence negating the other mechanisms mentioned in the Introduction is given in Table 5.

A possible thermally-activated mechanism for overcoming the Peierls-Nabarro stress (energy) is that mechanism originally proposed by Seeger (Ref. 44) to explain the Bordoni peak in f. c. c. metals, which is shown in Fig. 28. It involves the formation of a pair of kinks in a dislocation line lying in a close-packed direction by the combined action of thermal fluctuations and the applied stress, and the subsequent lateral propagation of the kinks along the dislocation line, resulting in the forward motion of the

Table 5. Evidence Against Specific Mechanisms Proposed as Rate-Controlling During the Low Temperature Deformation of the B. C. C. Metals

Mechanism	Contrary Evidence
Breaking-away from an interstitial atmosphere	<p>All yielding and flow phenomena exhibit the same values of H and v^*.</p> <p>H and v^* are independent of interstitial content.</p> <p>H and v^* are the same for the mobility of dislocations as determined by etch pits as for initial yielding.</p>
Nonconservative motion of jogs	<p>H and v^* are independent of structure.</p> <p>H and v^* for yielding and flow are the same as for the mobility of edge dislocations, which do not move nonconservatively.</p>
Overcoming interstitial precipitates	<p>H and v^* are independent of impurity content.</p> <p>H and v^* are independent of the quantity of interstitial precipitates.</p> <p>τ^* decreases with increase in quantity of precipitates.</p>
Cross-slip.	<p>H and v^* for yielding and flow are the same as for the mobility of edge dislocations, which cannot cross-slip.</p>

dislocation. Seeger (Ref. 44) calculated the activation energy for this process at low stresses to be

$$H = H_K \left[1 + \frac{1}{4} \log \left(\frac{16\tau_p^0}{\pi\tau^*} \right) \right]^\dagger \quad (7)$$

where H_K is the energy of a single kink, and τ_p^0 is the Peierls-Nabarro stress at 0°K . Furthermore, Seeger gives

$$H_K = \frac{2a}{\pi} \left(\frac{2E_0 ab\tau_p^0}{\pi} \right)^{1/2} \quad (8)$$

and

$$H_{PN} = \frac{\tau_p^0 ab^2}{2\pi} \quad (9a)$$

$$= \frac{H_K^2 \pi^2 b}{16a^2 E_0} \quad (9b)$$

where $2H_{PN}$ is the Peierls-Nabarro energy per atomic length, a is the distance between close-packed rows, b is the Burgers vector, and E_0 is the line energy of a dislocation. Taking the average value of τ_p^0 (from Table 2) for T_p^0 and taking $E_0 = 1/2 \mu b^2$, one obtains from Eqs. (7) and (8), H_0 ($\tau^* = 1 \text{ kg/mm}^2$) $\approx 0.1 \mu b^3$, which is in good agreement with measured values of H_0 , Table 6. Furthermore, from Eqs. (7) and (8), $H_K = 3-4 \times 10^{-2} \mu b^3$

[†]The thermal component of the stress τ^* has been substituted for the total stress τ in Seeger's equation.

and from Eq. 9, $H_{PN} = 1.2 \times 10^{-3} \mu b^3$, Table 6. Taking the derivative of Eq. 7 with respect to τ^* gives

$$-\frac{dH}{d\tau^*} = v^* = \frac{1}{4} \frac{H_K}{\tau^*} \quad (10)$$

Values of H_K derived from the values of v^* at $\tau^* = 1 \text{ kg/mm}^2$ are also given in Table 6 and are in agreement with those obtained from Eqs. (7) and (8). For comparison, values of H_K derived from the slope of the plots of H vs $\log \tau^*$ (Fig. 20) at low stresses ($< 1 \text{ kg/mm}^2$) are approximately 1/6 to 1/3 those calculated using Eqs. (7) and (8), while those derived from the slope at high stresses ($> 10 \text{ kg/mm}^2$) are about 3 to 4 times larger. Agreement occurs in the intermediate stress range ($\tau^* = 1-5 \text{ kg/mm}^2$), where the plots show curvature.

The good agreement between the values of H_o and H_K obtained from the various relationships, Eqs. (7)-(10) indicates rather strongly that the nucleation of kinks is the rate-controlling mechanism during low temperature deformation of the b. c. c. metals. Although the derived values of τ_p^o , H_K and H_{PN} are somewhat higher than those usually given for close-packed metals (Ref. 45), they are in accord with those calculated using the original Peierls-Nabarro equations (Ref. 46) and the more recent calculations of Kuhlmann-Wilsdorf (Ref. 47) and Hobart and Celli (Ref. 48). The good agreement between the values of H_o and H_K obtained using only experimental data and those obtained using $E_o = 1/2 \mu b^2$ indicates that the line energy in the b. c. c. metals is very nearly $1/2 \mu b^2$.

According to Seeger (Ref. 44) the width, w , of a kink is given by

$$w = \frac{1}{2} a \left(\frac{E_o b}{H_{PN}} \right)^{1/2} \quad (11)$$

Table 6. Values of H_O , H_K , and H_{PN} Derived from the Experimental Data

Metal	b Å	μb^3 ergs $\times 10^{-12}$	H_O ($\tau^* = 1 \text{ kg/mm}^2$)/ μb^3		$H_K/\mu b^3$		$H_{PN}/\mu b^3$	
			Eqs. (7) & (8) $\times 10^{-2}$	Figs. 12-18 $\times 10^{-2}$	Eq. (7) $\times 10^{-2}$	Eq. (8) $\times 10^{-2}$		Eq. (10) $\times 10^{-2}$
V	2.63	9.4	9.5	9.3	3.8	3.9	4.2	1.9
Nb	2.86	9.5	10.7	9.3	3.8	4.4	4.5	2.4
Ta	2.86	16.6	8.9	9.3	3.8	3.6	5.5	1.6
Cr	2.50	17.6	7.8	8.5	3.3	3.1	3.7	1.2
Mo	2.73	25.5	7.6	8.3	3.3	3.0	4.1	1.1
W	2.73	31.5	8.4	8.2	3.2	3.2	4.1	1.3
Fe	2.48	11.2	7.8	8.3	3.4	3.2	2.7	1.3

$\mu = 3/8E$, where E is Young's modulus at 300°K (Tietz and Wilson, Ref. 30).

and the critical separation, l^* , of the kinks during thermal activation is

$$l^* = \frac{w}{\pi} \log \left(\frac{32H_{PN}}{\tau^* b^3} \right) \quad (12a)$$

$$= \frac{H - H_K}{2H_{PN}} \quad (12b)$$

The values of w and of l^* (at $\tau = 1 \text{ kg/mm}^2$) obtained from Eqs. (11), (12a), and (12b) using the average values of H_K , H_{PN} , and H ($\tau^* = 1 \text{ kg/mm}^2$) from Table 6 and taking $E_0 = 1/2\mu b^2$, are given in Table 7. It is here seen that $w = 7-10 b$ and $l^*(\tau^* = 1 \text{ kg/mm}^2) = 12-22 b$, which are quite reasonable. Again, of significance is the good agreement between values of l^* from Eqs. (12a) and (12b).

Table 7. Values of w and l^* Derived from the Experimental Data

Center	w/b	l*/b	
		Eq. (12a)	Eq. (12b)
V	8	15	14
Nb	8	15	12
Ta	9	17	13
Cr	10	19	20
Mo	11	21	20
W	10	21	18
Fe	10	18	19

For the Peierls-Nabarro mechanism, the frequency factor can be given by

$$\nu = \rho b \left[\left(\frac{1}{l^*} \right) (Lb) \left(\frac{b}{l^*} v_d \right) \right] \quad (13)$$

where ρ is the density of dislocations participating in the deformation, b the Burgers vector, l^* the length of dislocation segment involved in the thermal activation, L the maximum lateral spread of the kinks, and v_d the Debye frequency. The first term within the brackets represents the number of places per unit dislocation length where thermal fluctuations may nucleate a loop of length l^* ; the second term is the area of the slip plane swept out per successful thermal fluctuation; the third term is the frequency of vibration of a segment of length l^* . Taking $\rho = 10^9 \text{ cm}^{-2}$, $l^* = 10b$, $L = 10^{-4} \text{ cm}$ and $v_d = 10^{13} \text{ sec}^{-1}$, one obtains $\nu = 10^8 \text{ sec}^{-1}$, which is in agreement with that observed experimentally for many materials, Tables 3 and 4.

Since H and v^* as a function of τ^* were independent of structure, the effect of impurities, precipitates, grain size, dislocations, and other aspects of previous thermal or mechanical history on the temperature dependence of the yield or flow stress is then due to a change in the frequency factor, ν , i. e., in the number of dislocations, ρ , participating in the deformation or in the lateral distance, L , a kink can move before encountering an obstacle. In this regard, Conrad and Frederick (Ref. 8) investigated the effect of straining and of interstitial precipitates in iron on the temperature dependence of τ^* . Some of their results are given in Fig. 3, which shows that a weaker temperature dependence results from straining and from the presence of precipitates. In Figs. 29 and 30 (from Ref. 8) it is shown that the weaker temperature dependence is associated with a larger value of ν , given by the slope of the plot of H vs temperature. From the relation $\nu = \rho b s v^*$ and taking the value of $s v^*$ derived from the dislocation velocity measurements of Stein and Low (Ref 49), they obtained values of ρ , and their increase with strain (Table 8) in agreement with dislocation densities determined by Keh

and Weissman (Ref. 42) by thin-film electron microscopy, indicating that the increase in ν was due primarily to an increase in ρ . They further concluded from their results that precipitates represented good sources for dislocations, which is in agreement with observations of Leslie (Ref. 50) and Van Torne and Thomas (Ref. 51).

Table 8. Effect of Strain on the Dislocation Density Participating in the Plastic Flow of Iron Determined from the Frequency Factor ν (Ref. 8)

Material	Strain	ν , Sec ⁻¹	ρ , cm ⁻²
Vacuum Melted Electrolytic Iron, Water Quenched from 920°C	1×10^{-3}	2.1×10^7	8.4×10^8
	5×10^{-2}	8.2×10^7	3.3×10^9
Ferrovac, Decarburized	2×10^{-2}	3.8×10^6	1.5×10^8
	10×10^{-2}	1.7×10^8	6.6×10^9
	20×10^{-2}	5.3×10^9	2.1×10^{11}
Ferrovac, Annealed	$> 5 \times 10^{-2}$	5.3×10^9	2.1×10^{11}

From Table 3 it is seen that the weaker temperature dependence of τ^* for single crystals or pure polycrystals, as compared to impure polycrystals in the Group VIA metals and iron, is associated with a frequency factor that is larger by 3 to 5 orders of magnitude. These larger values of ν cannot be due entirely to a greater dislocation density, ρ , because this would require unreasonably large values for ρ . Rather, it appears that this difference in ν is primarily due to larger values of L for the pure as compared to the impure materials, suggesting that interstitial atoms or precipitates influence the extent to which the kinks can spread before encountering an obstacle. Besides acting as obstacles to kink motion, the interstitial atoms or precipitates may induce cross-slip, which in turn limits the dislocation loop length

on the slip plane. Of interest in this regard are the observations of Schadler and Low (Ref. 19), who report that under some conditions dislocations in tungsten crystals can move long distances without multiplying, in agreement with the high values of ν given in Table 3 for single crystals of tungsten.

All of the above supports overcoming the Peierls-Nabarro stress by thermally-activated nucleation of kinks as the rate-controlling mechanism in the b. c. c. metals at low temperatures. However, explanation is needed for the fact that in the vicinity of T_0 (i. e., $\tau^* = 0$) H , for the most part, does not increase as rapidly with decrease in stress (or increase in temperature) as is expected from the values of ν^* or the straight line portion of the H versus temperature curves at lower temperatures. As indicated earlier, the scatter in the data allows for a more rapid increase in H than is indicated by the curves drawn in Figs. 12-18. The low values of H for stresses only slightly greater than zero may then simply reflect the difficulty in defining $\tau^* = 0$ exactly. Also, ν may actually decrease with increase in temperature (or decrease in stress).[†] On the other hand, a different mechanism may become rate-controlling in the very low stress range. Additional work is needed to resolve this problem.

Finally, one needs to explain the much smaller temperature dependence of the proportional limit after straining and the fact that σ_E , as defined by Brown and Ekvall (Ref. 15), is independent of temperature. Also, in recent investigations on the determination of H as a function of stress in Ta by creep tests, Chambers (Ref. 39) found a spectrum of activation energies for very small strain rates (10^{-6} - 10^{-11} sec⁻¹) rather than a single

[†]The change in ν may be the result of straining at different temperature (or stresses) rather than the effect of stress or temperature per se.

activation energy. † There are two possible explanations for these various effects:

First, these phenomena represent the motion of those specific dislocations located in the most favorable internal stress fields, and the applied stress primarily gives direction to the motion of these dislocations and does not contribute significantly to the thermally-activated process.

Second, another less difficult mechanism is rate-controlling at the very low stress levels, for example the lateral motion of kinks, as proposed by Brailsford (Ref. 52), or the lateral motion of jogs as suggested by Chambers. ††

In both cases the easier motion would soon die out, and to obtain gross macroscopic flow the more difficult mechanism of nucleating kinks would become rate-controlling. The rapid strain hardening associated with the early part of the stress-strain curve would then be an exhaustion hardening rather than an interaction hardening, which occurs subsequently during macroflow. Here, also, additional research is needed to resolve this question.

B. YIELD POINT AND WORK HARDENING

The fact that K in Eq. (1) is relatively independent of temperature and that the activation energy and activation volume as a function of stress are the same for all deformation phenomena suggests that the yield point in the b. c. c. metals is not due to the thermally-assisted unpinning of dislocations from their interstitial atmosphere, as proposed by Cottrell (Ref. 1), but results from the sudden multiplication of dislocations by the double cross-slip mechanism of Koehler (Ref. 53) and Orowan (Ref. 54), as proposed by Johnson and Gilman (Ref. 55) for LiF. In this latter model, the multiplication of dislocations is controlled by their motion through the lattice, which agrees

†As an upper limit, Chambers (Ref. 39) reported an H versus stress relationship in agreement with that given in Fig. 14.

††R. C. Chambers, private communication.

with the experimental facts. As mentioned previously (Ref. 16), three factors favor the occurrence of such a yield point in the b. c. c. metals:

First, there exists only a small number of dislocations which can contribute to the plastic flow, due to the pegging of the available dislocations by interstitial precipitates (as distinct from pinning by an interstitial atmosphere).

Second, the dislocation density contributing to the plastic flow increases very rapidly with strain. This is inherent in the double cross-slip mechanism for multiplication and has been observed experimentally in iron by Keh and Weissman (Ref. 42) and in molybdenum by Benson.[†]

Third, the change in stress for a given change in dislocation velocity, $(\partial\sigma/\partial \ln \dot{s})$ or $(\partial\sigma/\partial \ln \dot{\epsilon})$, is relatively large, Fig. 2.

To check the proposed interpretation of the yield point, stress-strain curves for mild steel were calculated (Ref. 16) using Eqs. (1) and (3) and the available information on the activation energy as a function of stress (Fig. 18), the value of sv^* derived from etch pit measurements in silicon-iron (Ref. 16), the increase in dislocation density with strain (Ref. 42), and the increase in flow stress associated with the increase in dislocation density (Ref. 42). The good agreement between the calculated and experimental curves is shown in Fig. 31. Since only plastic strain was considered, the upper yield point was taken as the stress at a plastic strain of 10^{-4} , which is approximately the observed pre-yield microstrain in iron and steel.

[†]R. Benson, private communication.

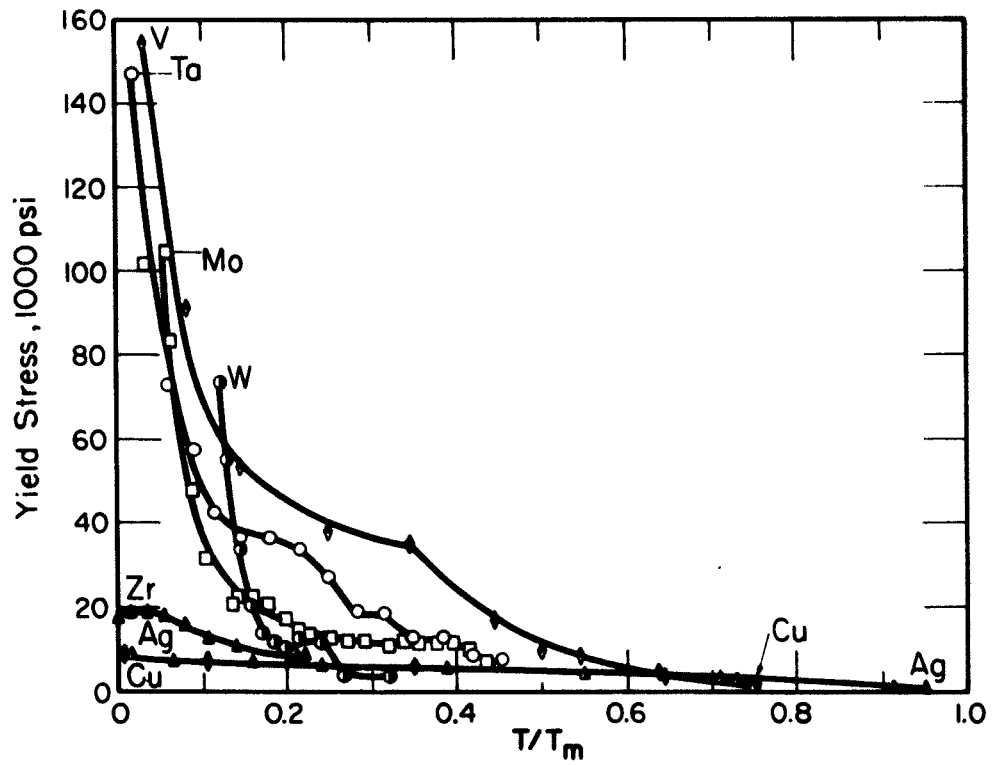


Fig. 1. Initial Yield Stress of Various Polycrystalline Metals vs Ratio of T/T_m

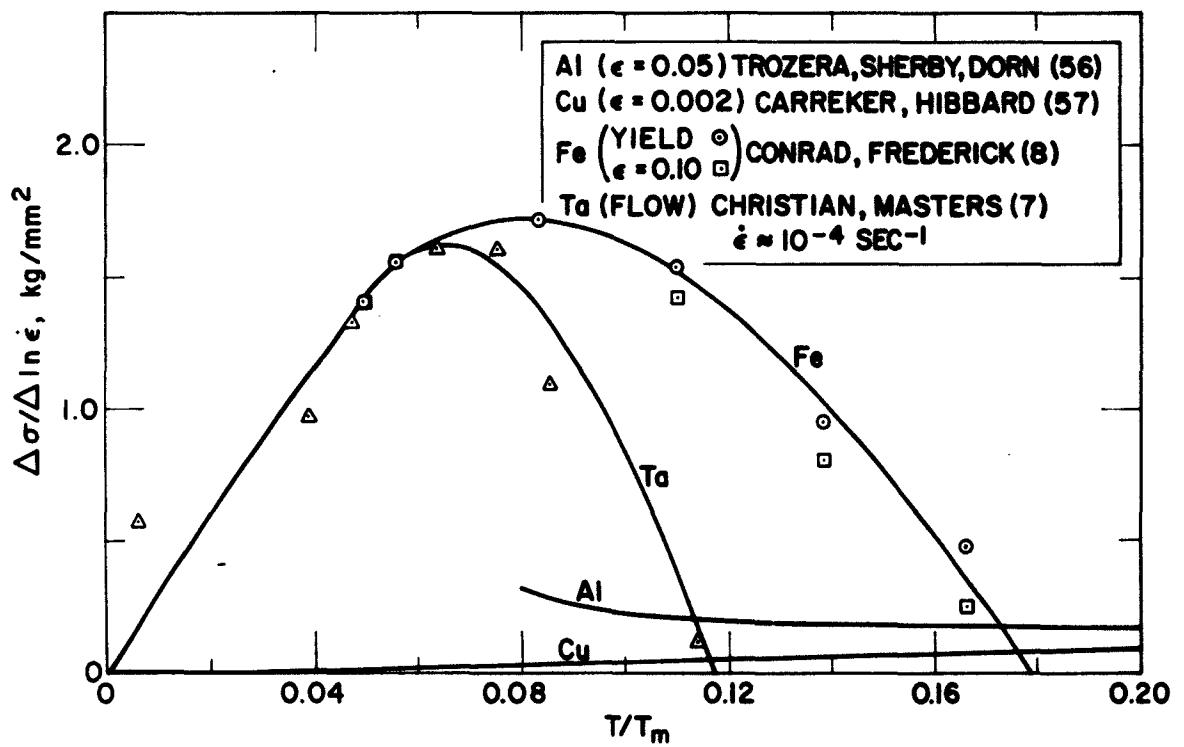


Fig. 2. Effect of Strain Rate on the Yield and Flow Stresses of F. C. C. and B. C. C. Metals

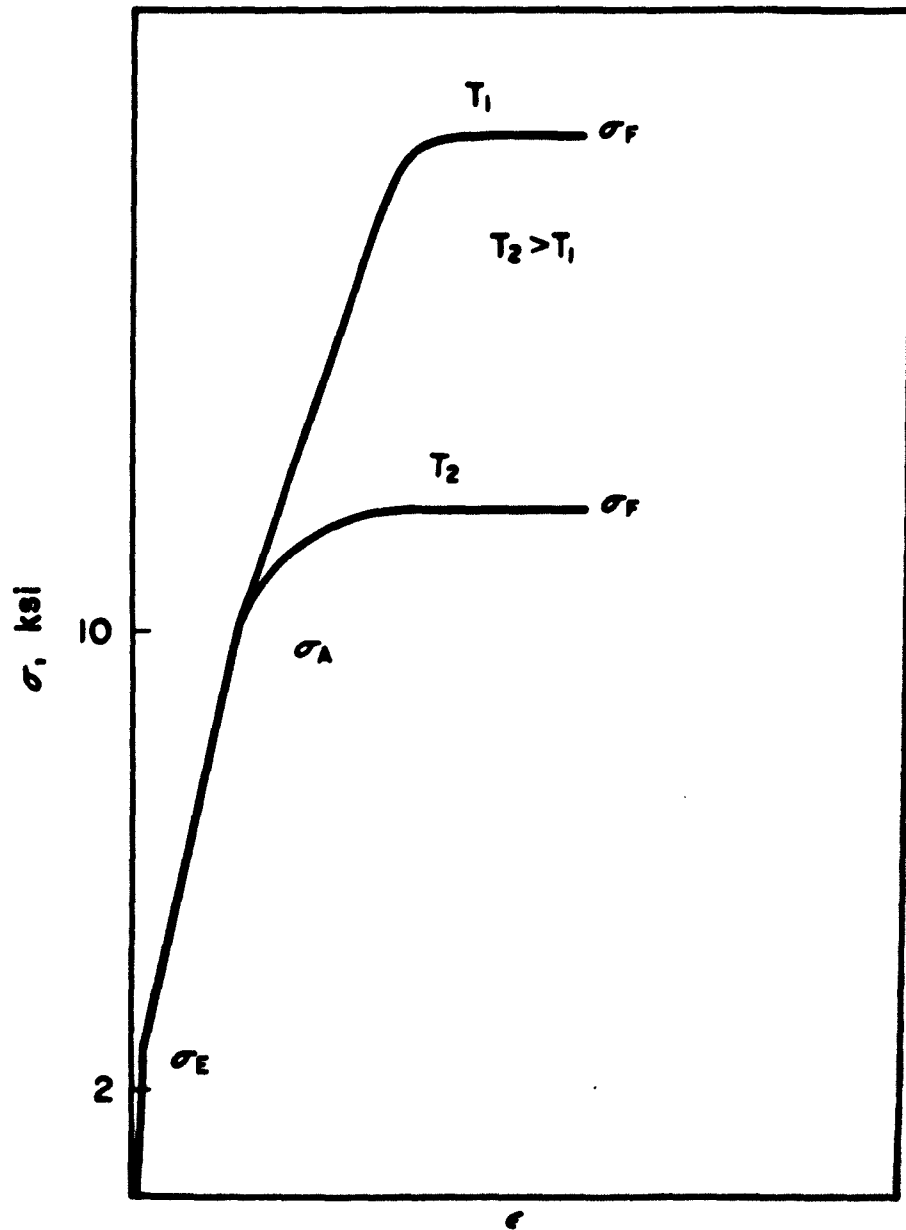


Fig. 3. Idealized Stress-Strain Curves for an Ultrapure Iron at Two Temperatures (from Brown and Ekvall, Ref. 15)

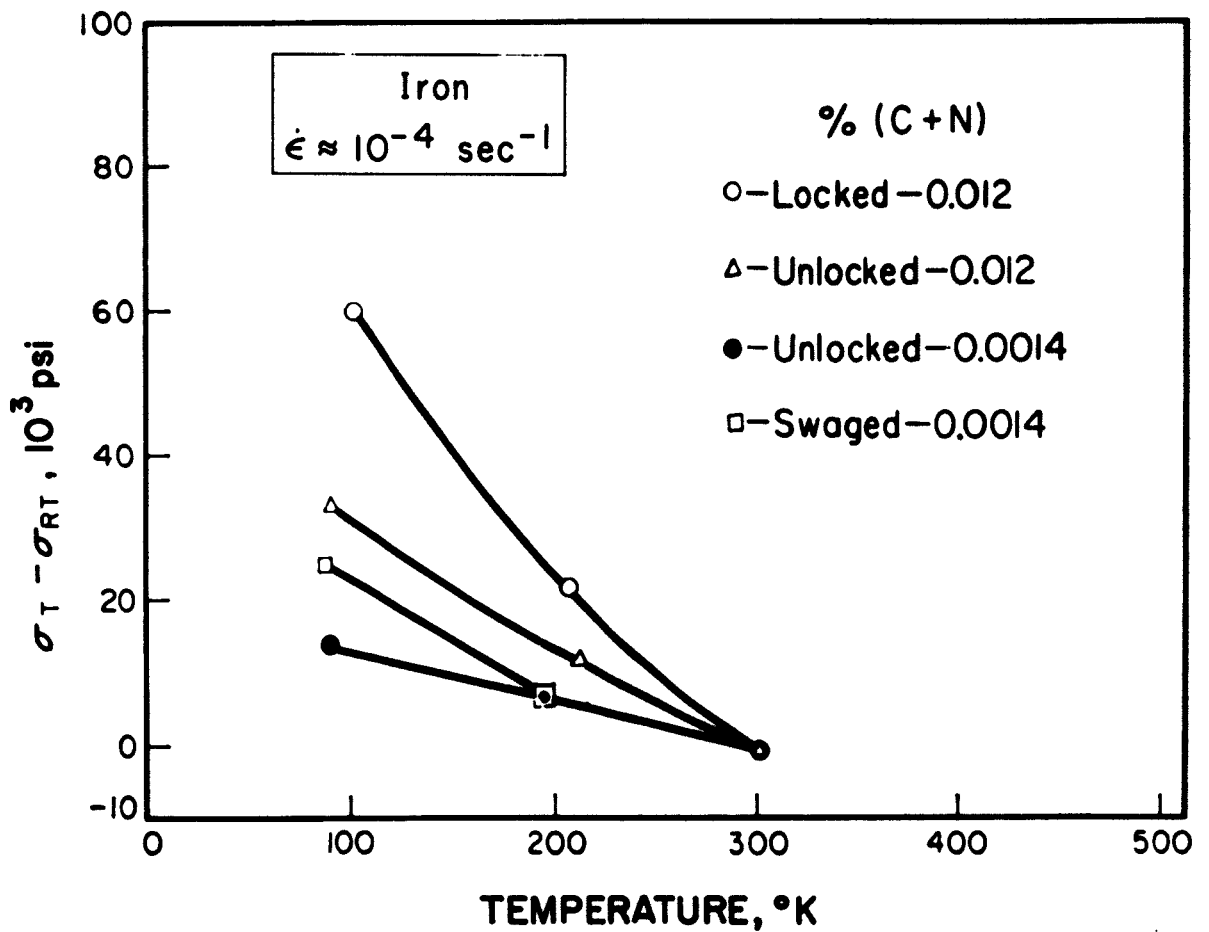


Fig. 4. Temperature Dependence of σ_A for Various Materials and States of Locking (from Brown and Ekvall, Ref. 15)

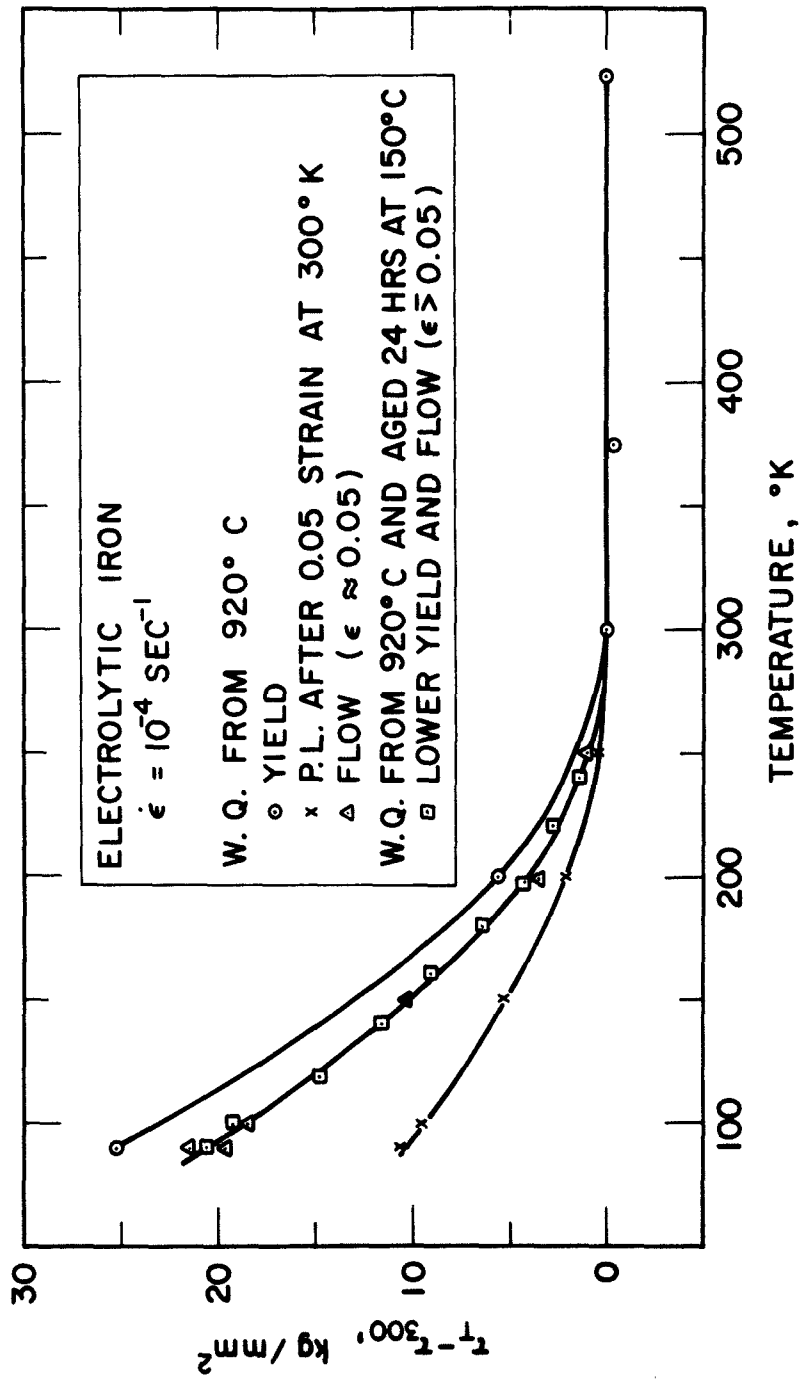


Fig. 5. Effect of Temperature on the Initial Yield Stress, the Proportional Limit After Straining, and the Flow Stress of Electrolytic Iron

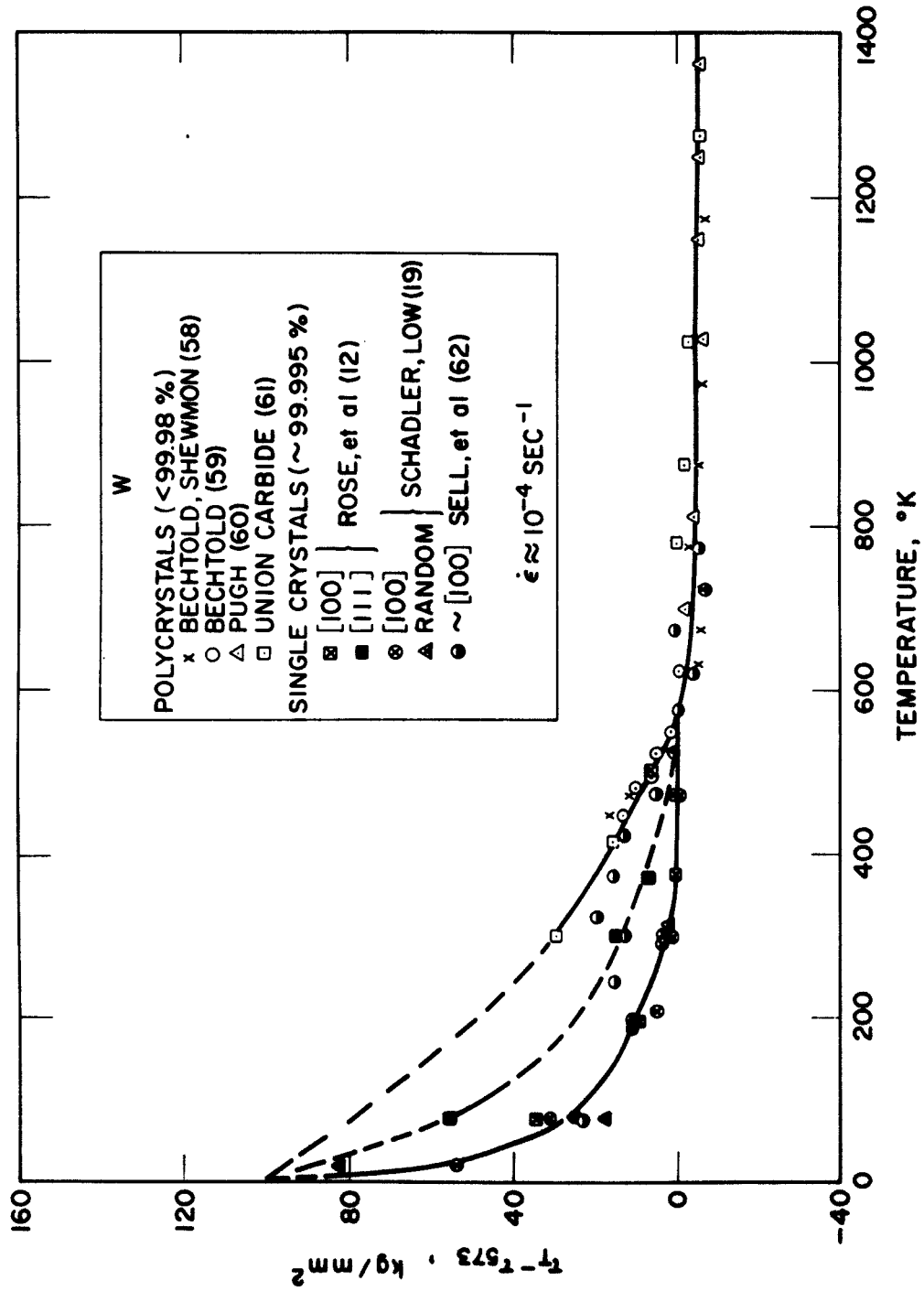


Fig. 6. Effect of Temperature on the Thermal Component of the Yield Stress of Tungsten

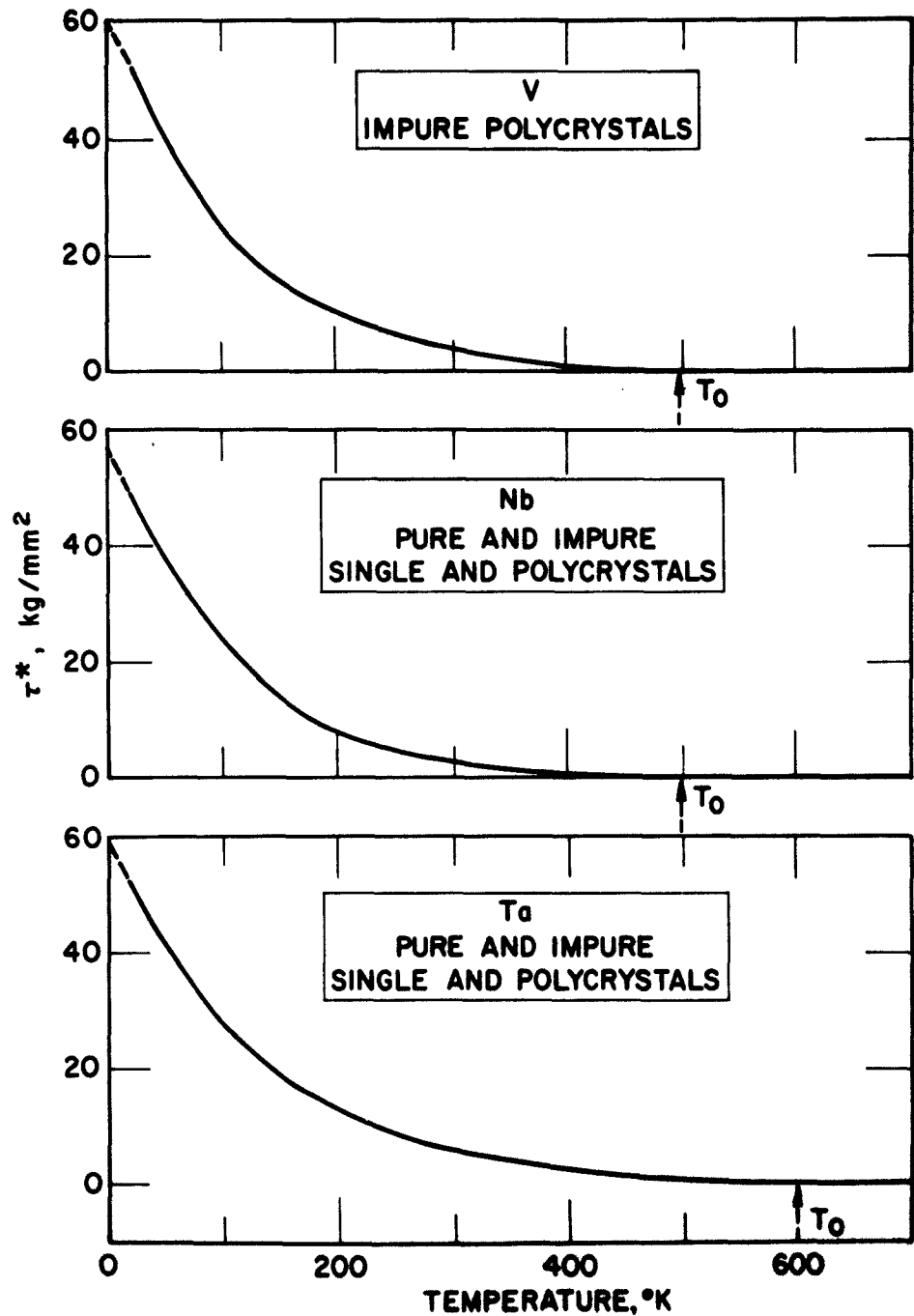


Fig. 7. Variation of τ^* with Temperature for Pure (<0.005 wt % Interstitials) and Impure (>0.02 wt % Interstitials) Group VA Metals, Strain Rate 10^{-4} sec^{-1}

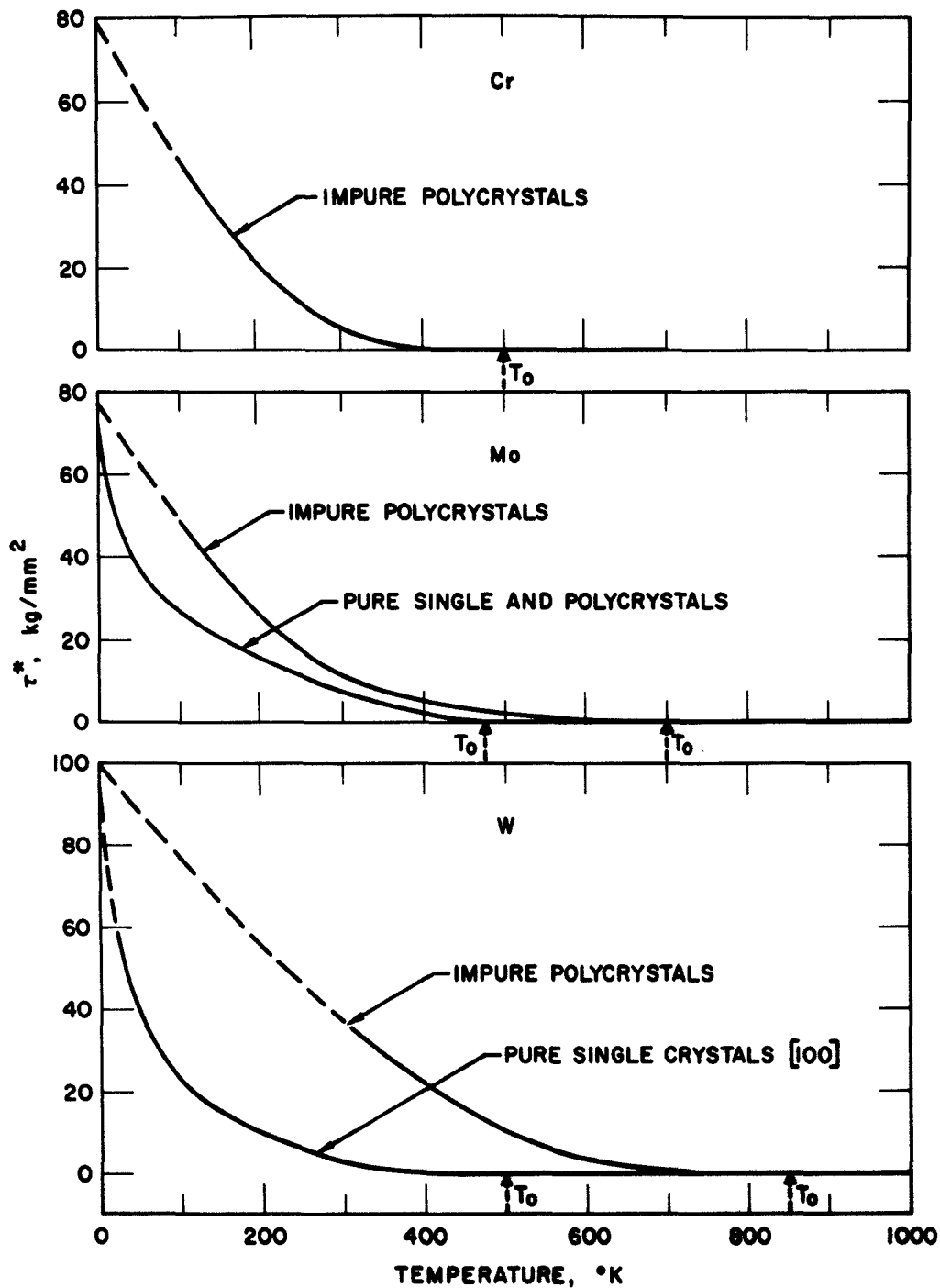


Fig. 8. Variation of τ^* with Temperature for Pure (<0.005 wt % Interstitials) and Impure (>0.02 wt % Interstitials) Group VIA Metals, Strain Rate 10^{-4} sec^{-1}

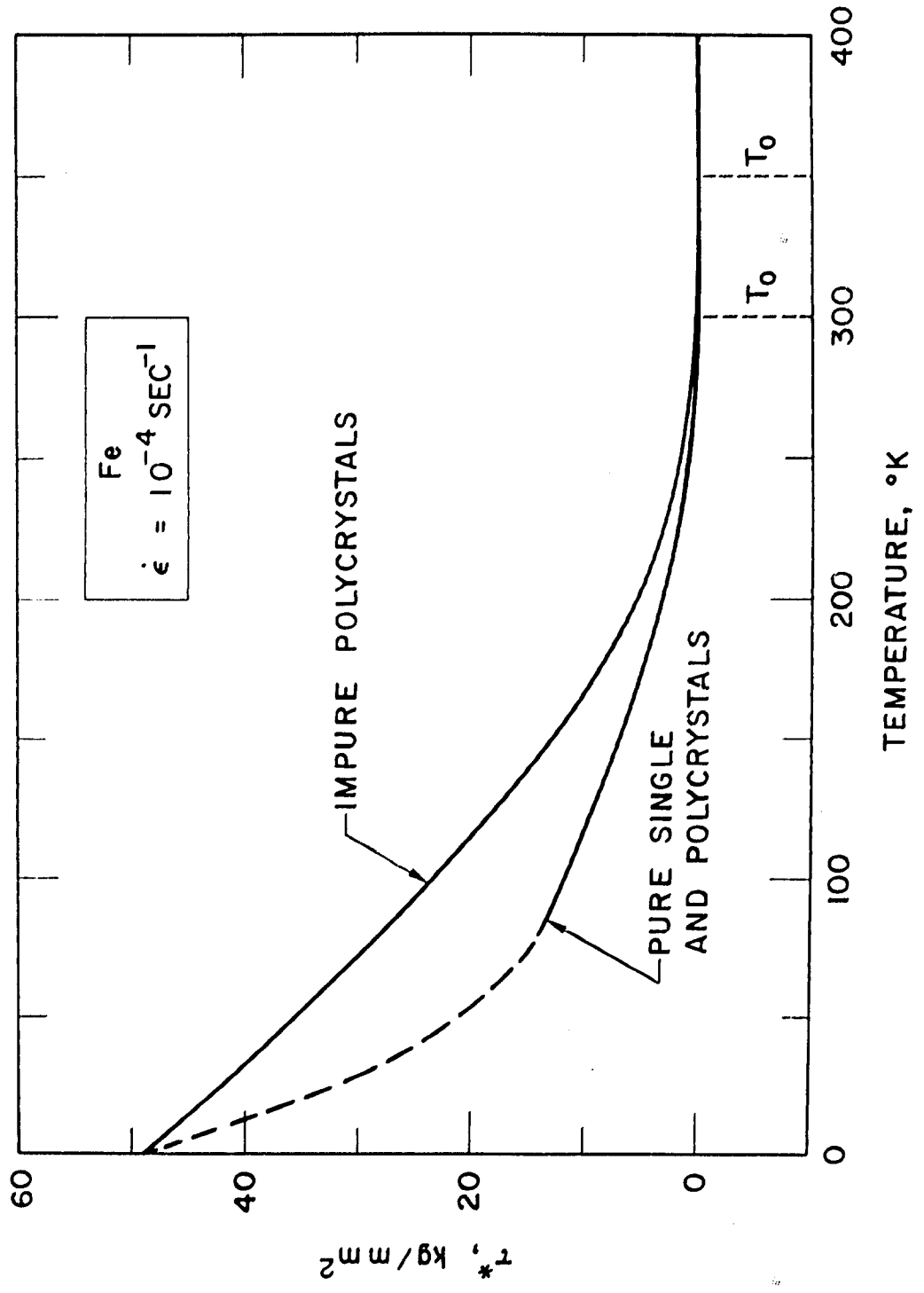


Fig. 9. Variation of τ^* with Temperature for Pure (<math><0.005\text{ wt \%}</math> Interstitials) and Impure (>0.02 wt % Interstitials) Iron

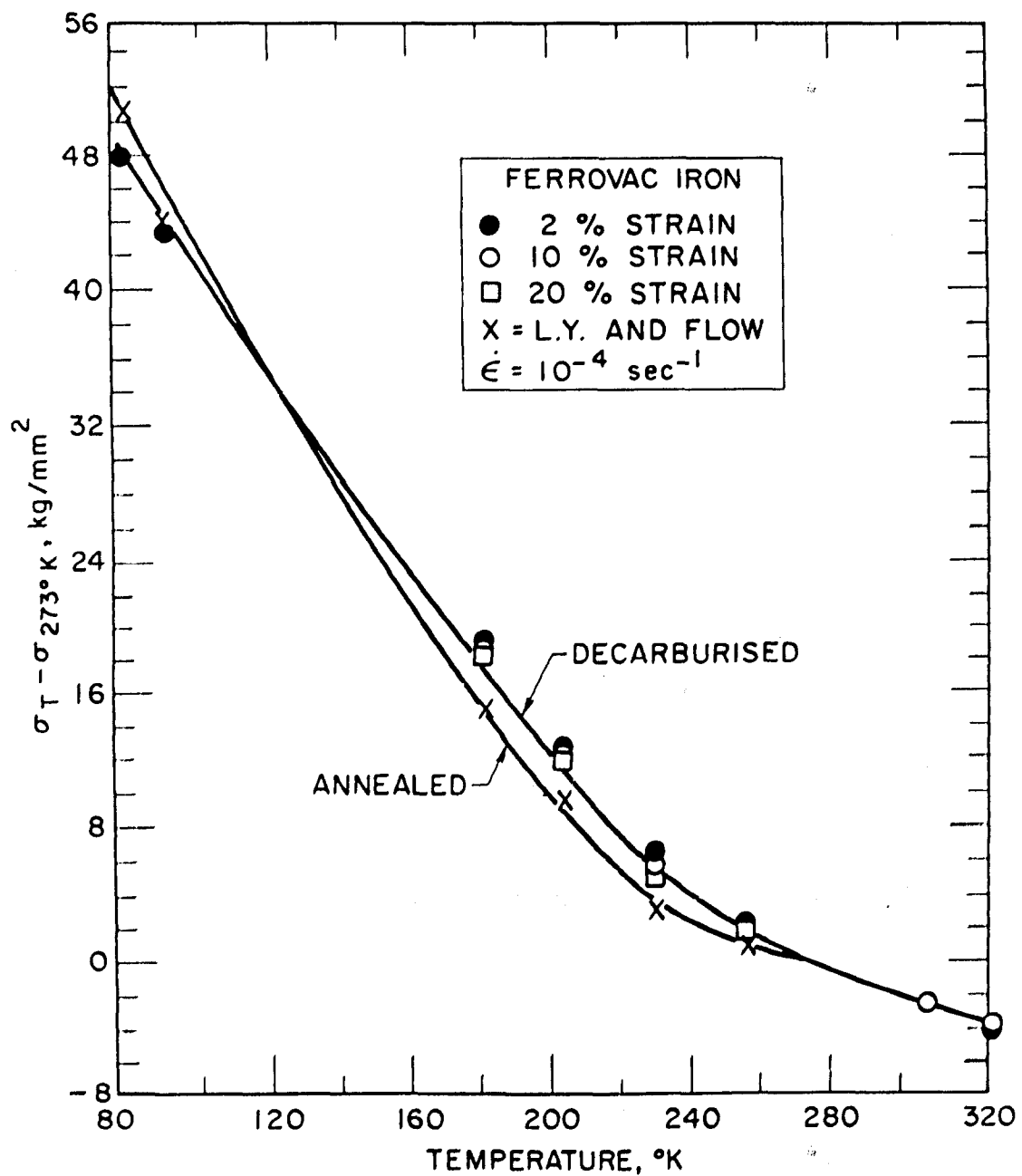


Fig. 10. Temperature Dependence of Reversible Flow Stress in Iron
(Data from Basinski and Christian, Ref. 5)

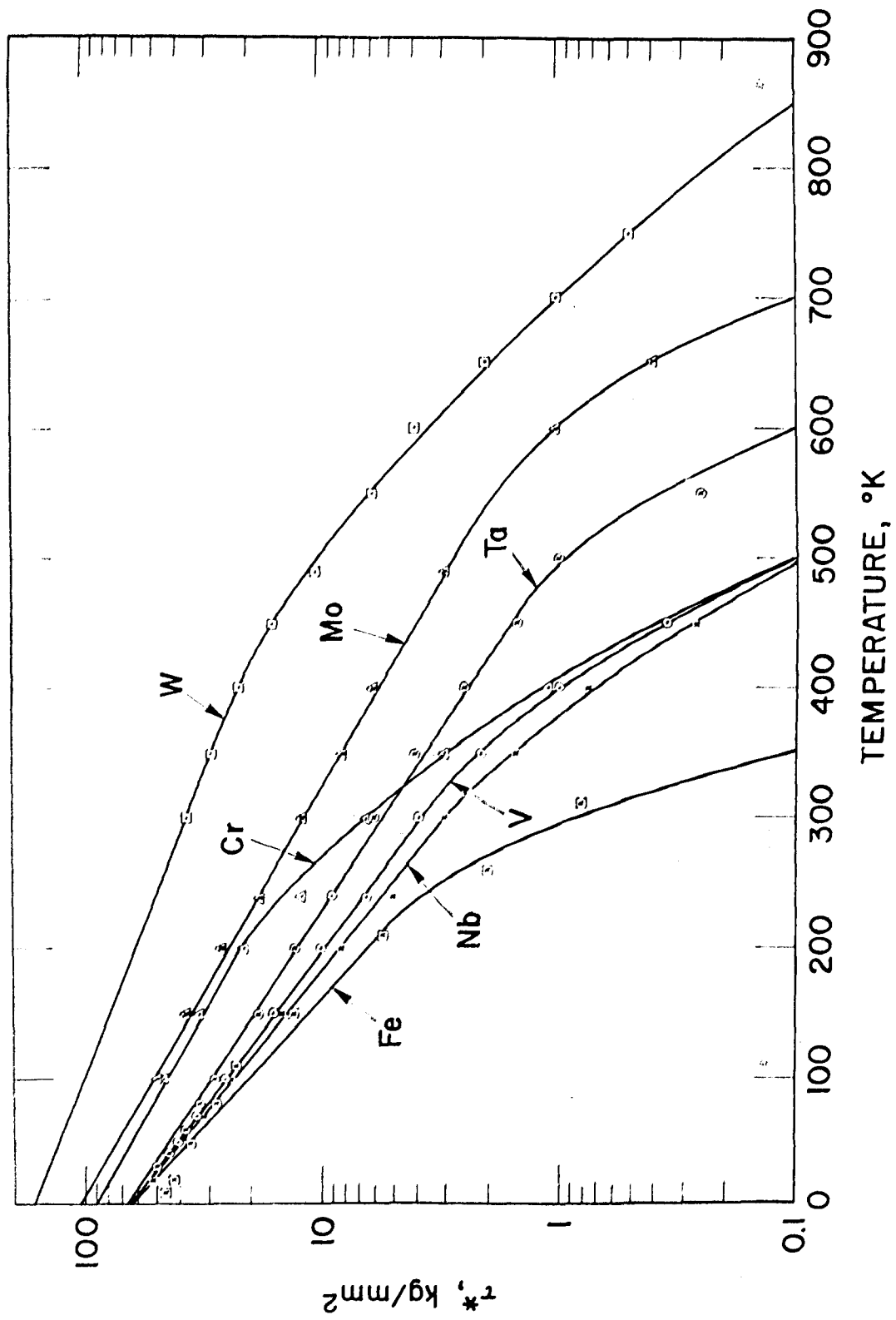


Fig. 11. Log τ^* vs Temperature for Impure Polycrystalline B. C. C. Metals

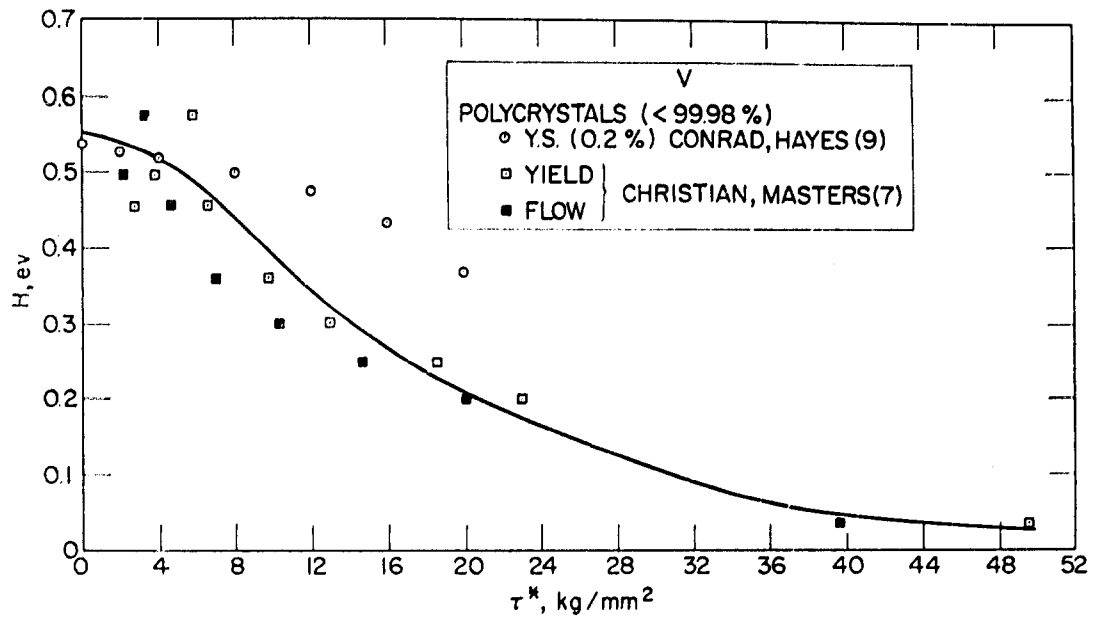


Fig. 12. Effect of Stress on the Activation Energy for the Deformation of Vanadium

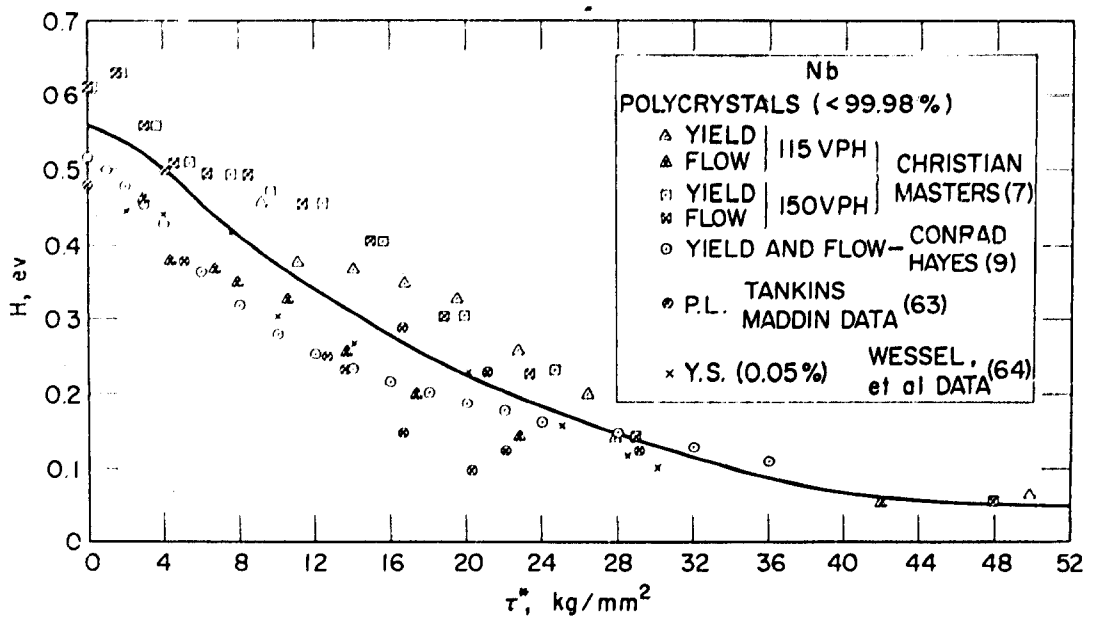


Fig. 13. Effect of Stress on the Activation Energy for the Deformation of Niobium

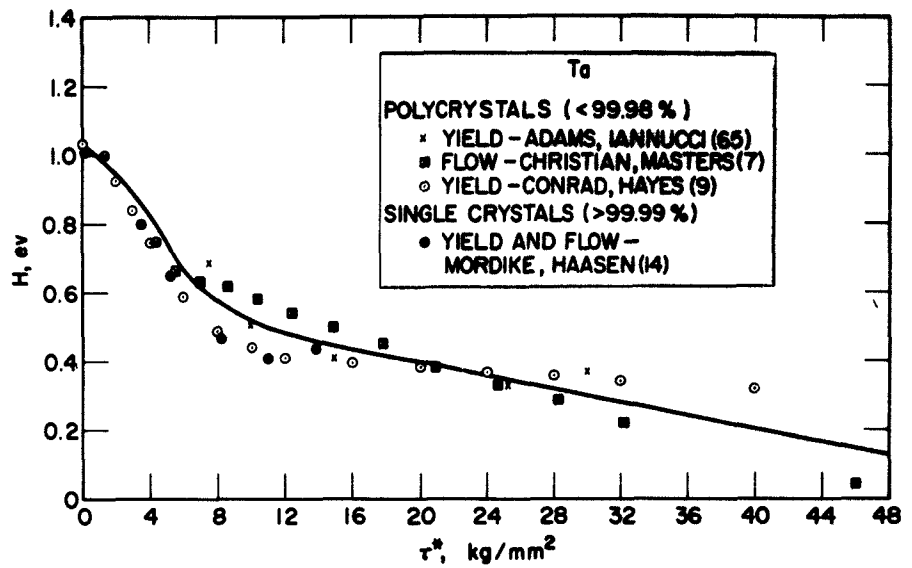


Fig. 14. Effect of Stress on the Activation Energy for the Deformation of Tantalum

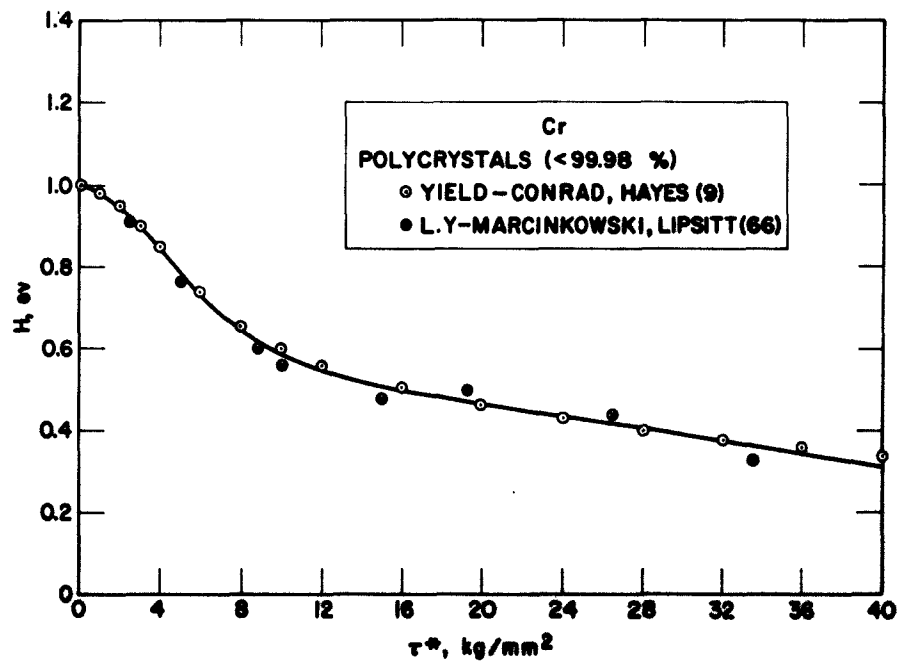


Fig. 15. Effect of Stress on the Activation Energy for the Deformation of Chromium

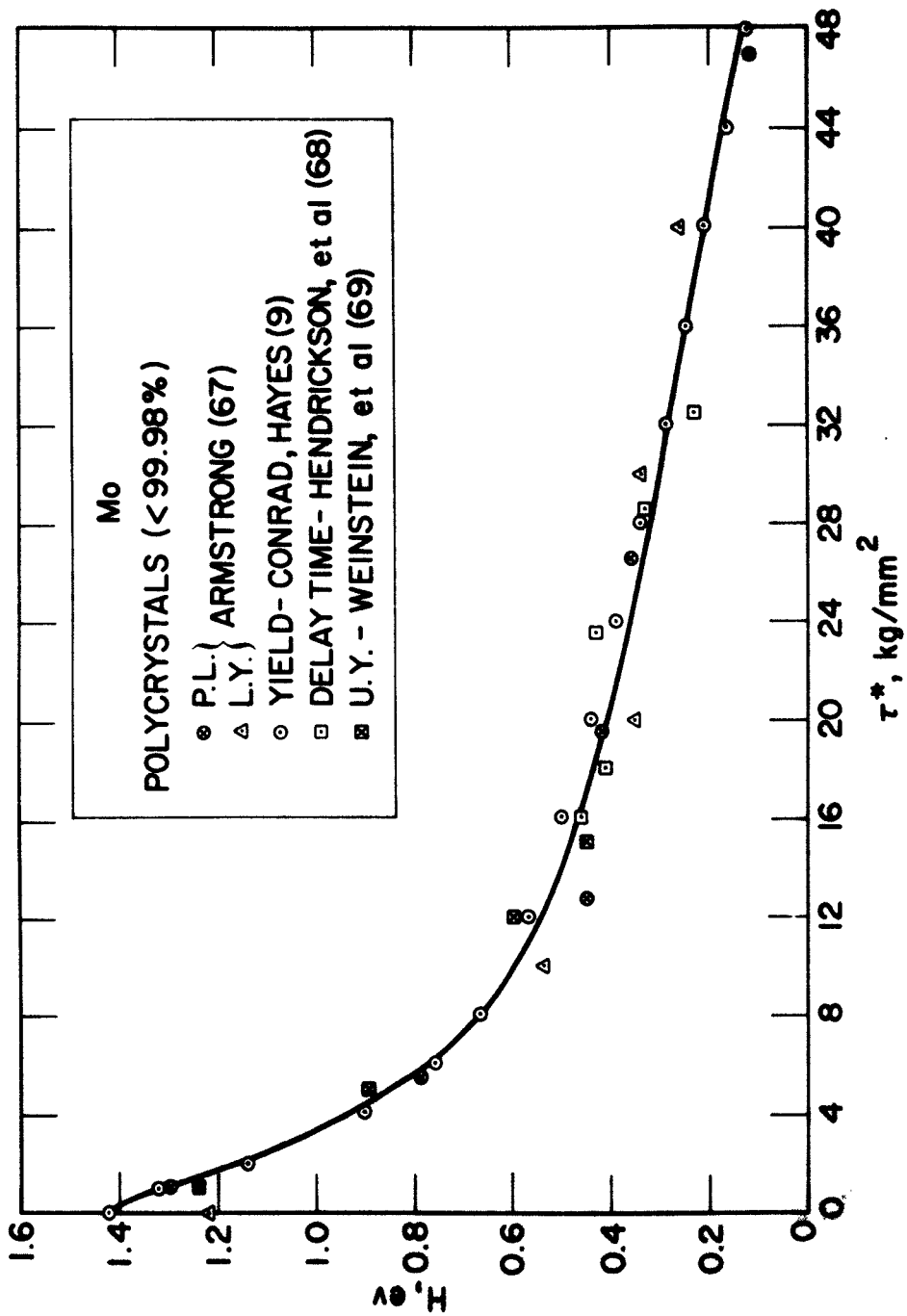


Fig. 16. Effect of Stress on the Activation Energy for the Deformation of Molybdenum

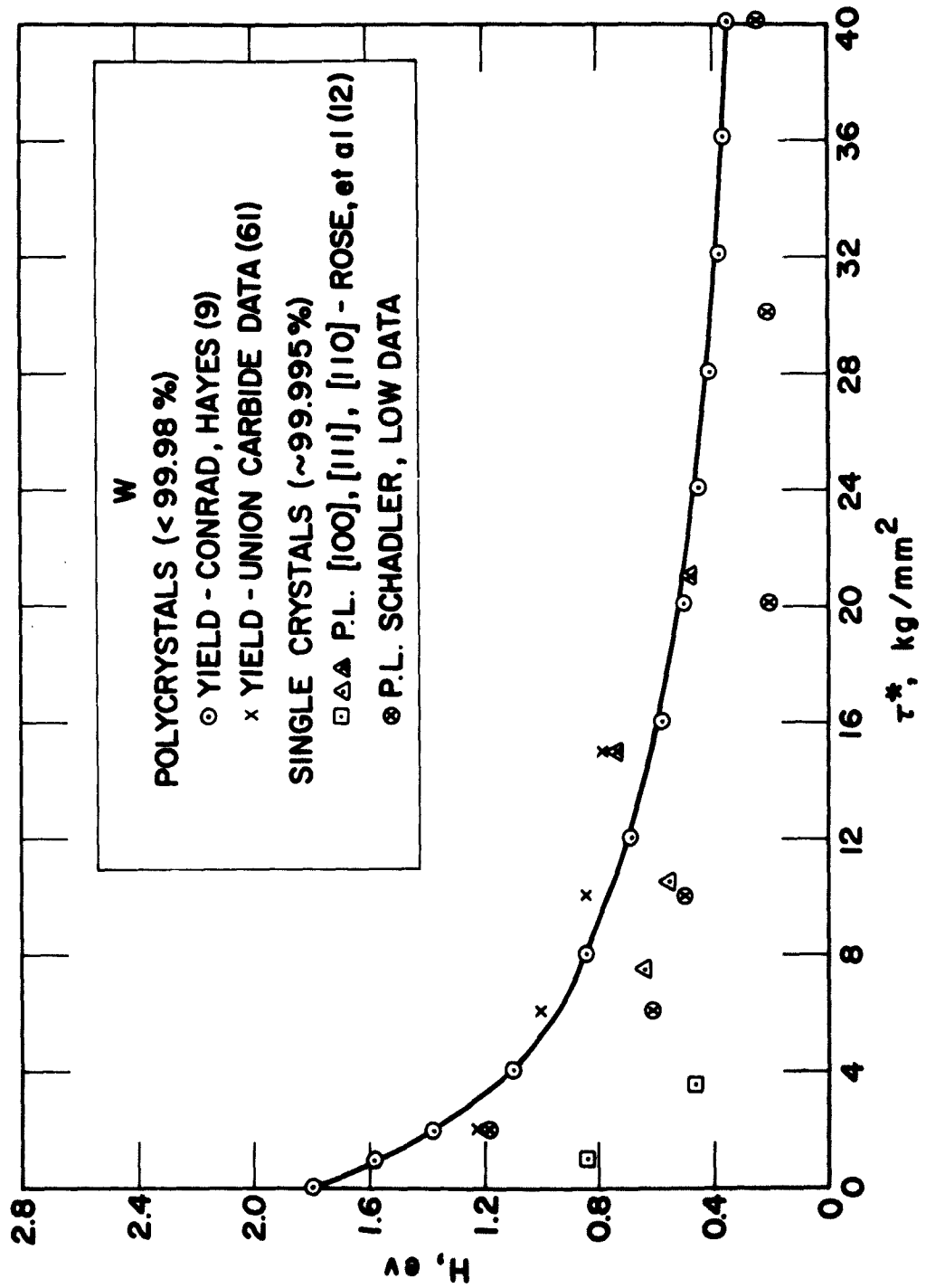


Fig. 17. Effect of Stress on the Activation Energy for the Deformation of Tungsten

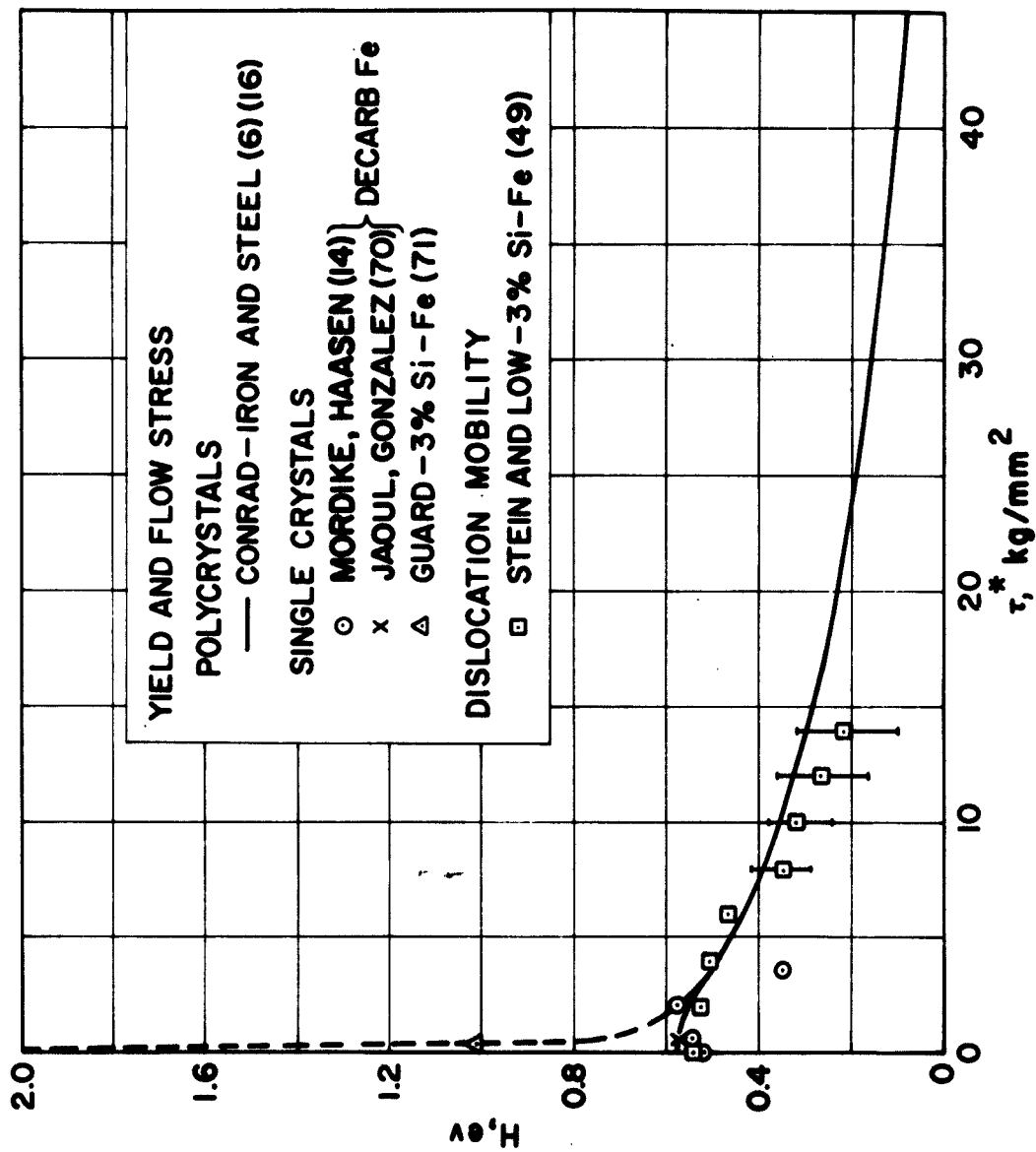


Fig. 18. Effect of Stress on the Activation Energy for Yielding and Flow in Iron and Steel

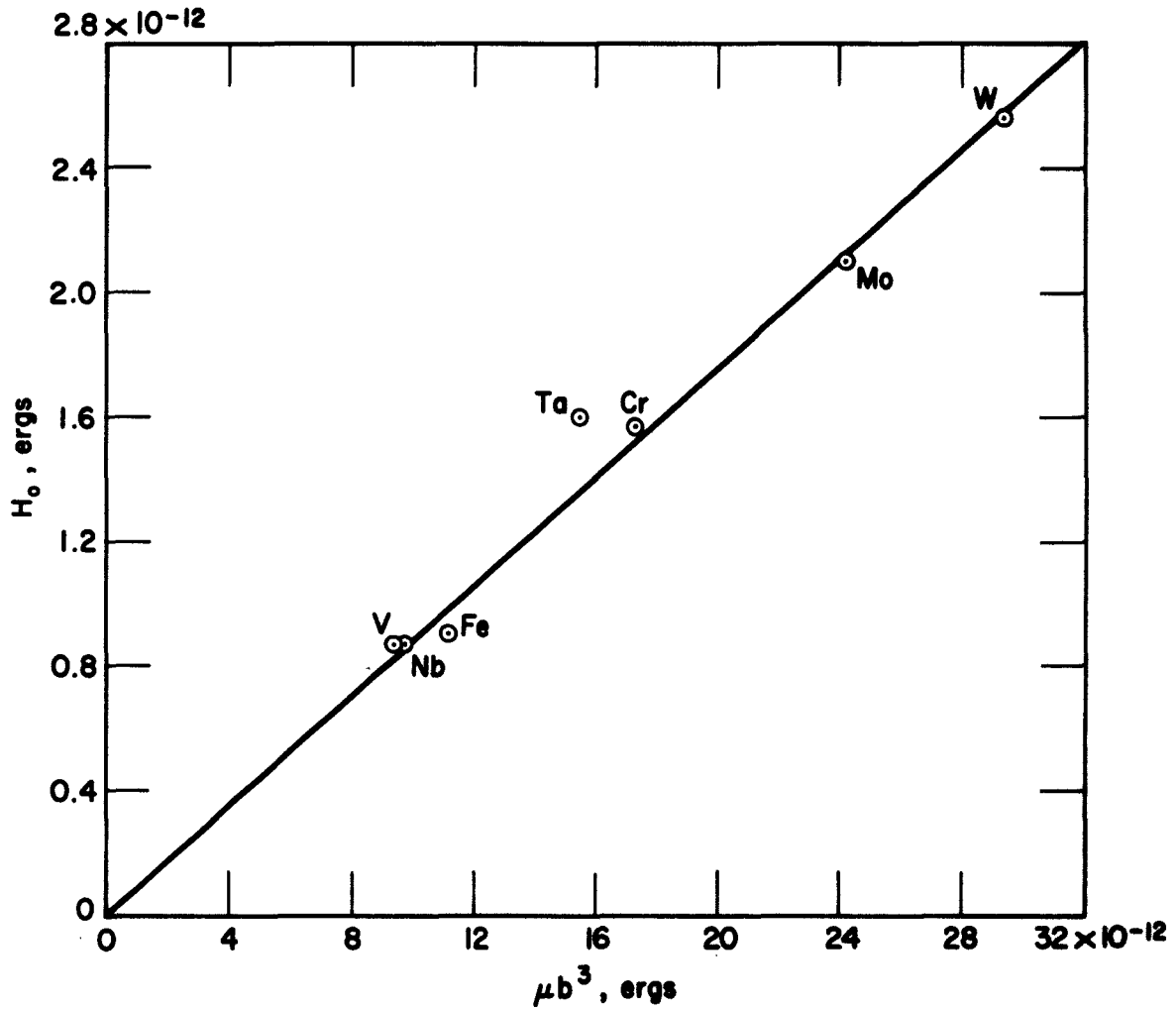


Fig. 19. Relationship Between H_0 ($\tau^* = 1 \text{ kg/mm}^2$) and μb^3 for the B. C. C. Metals

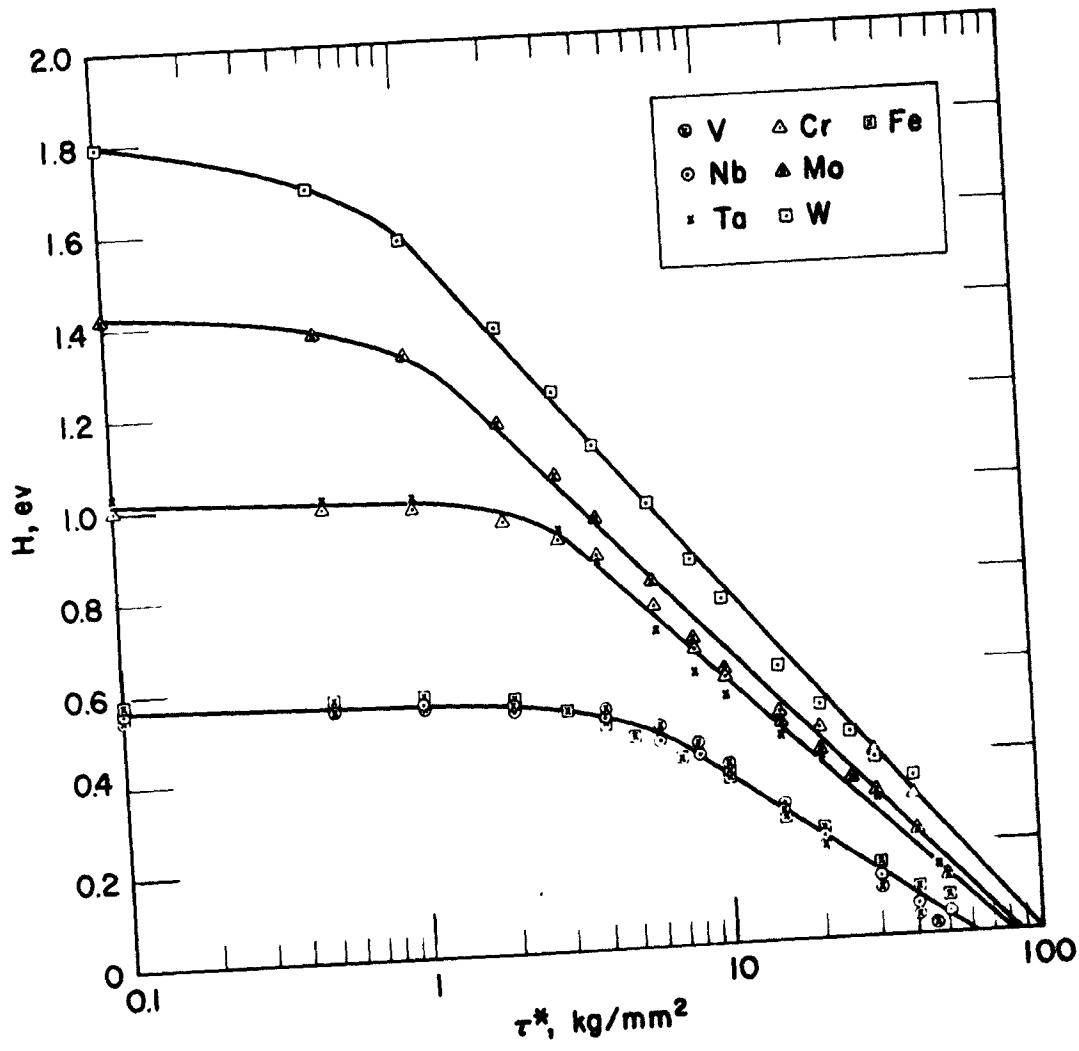


Fig. 20. Activation Energy vs Log τ^* for the B. C. C. Metals

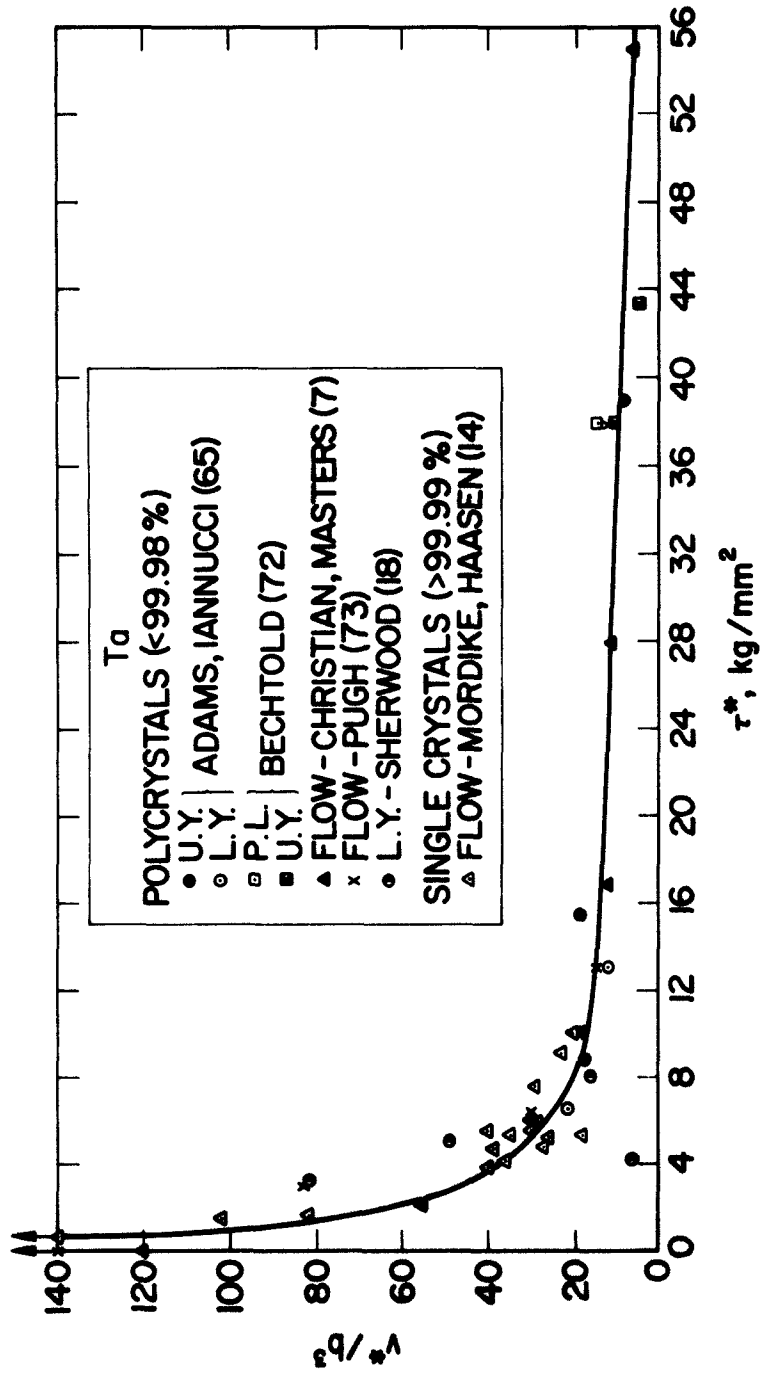


Fig. 21. Effect of Stress on the Activation Volume for the Deformation of Tantalum

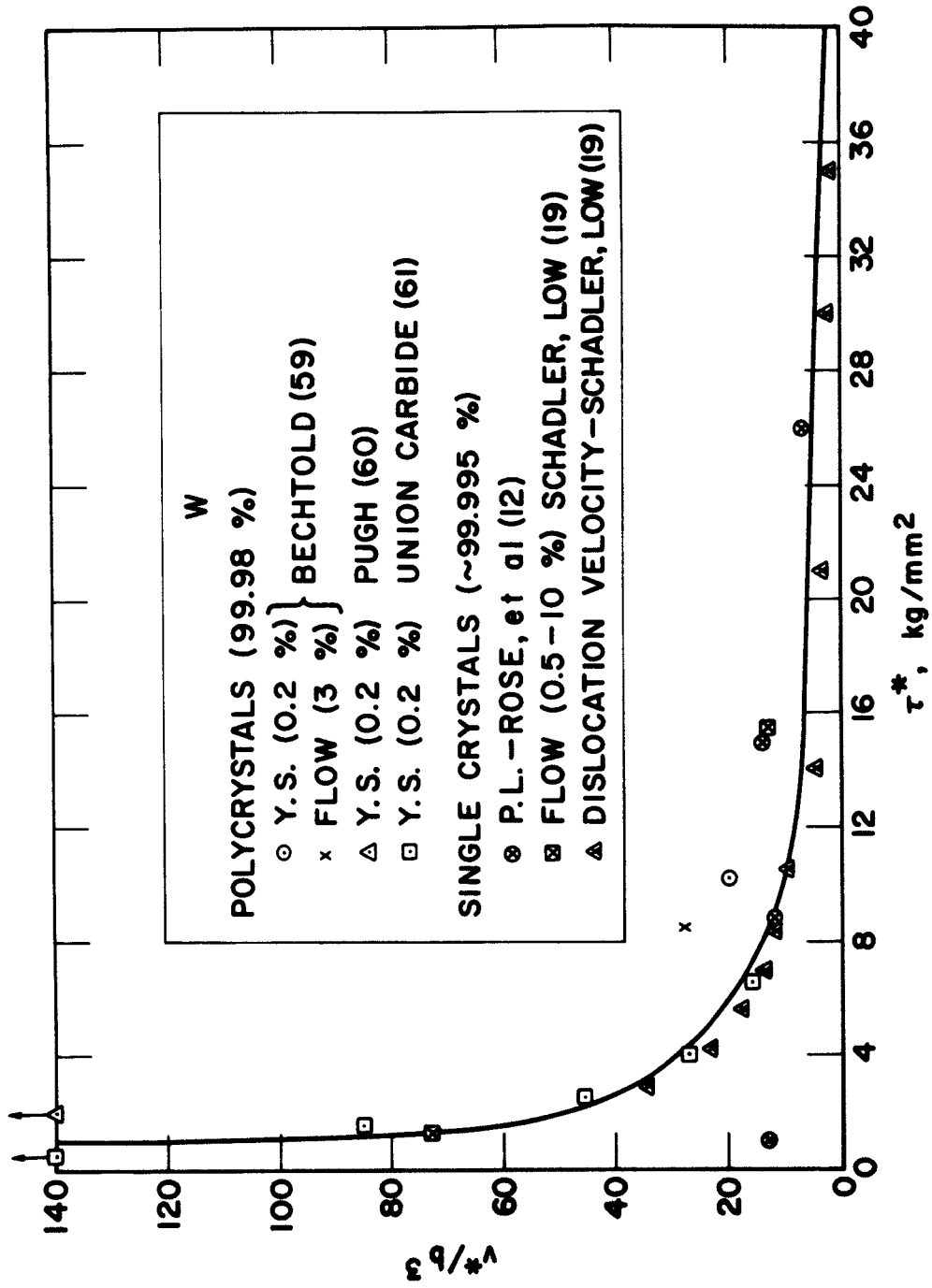


Fig. 22. Effect of Stress on the Activation Volume for the Deformation of Tungsten

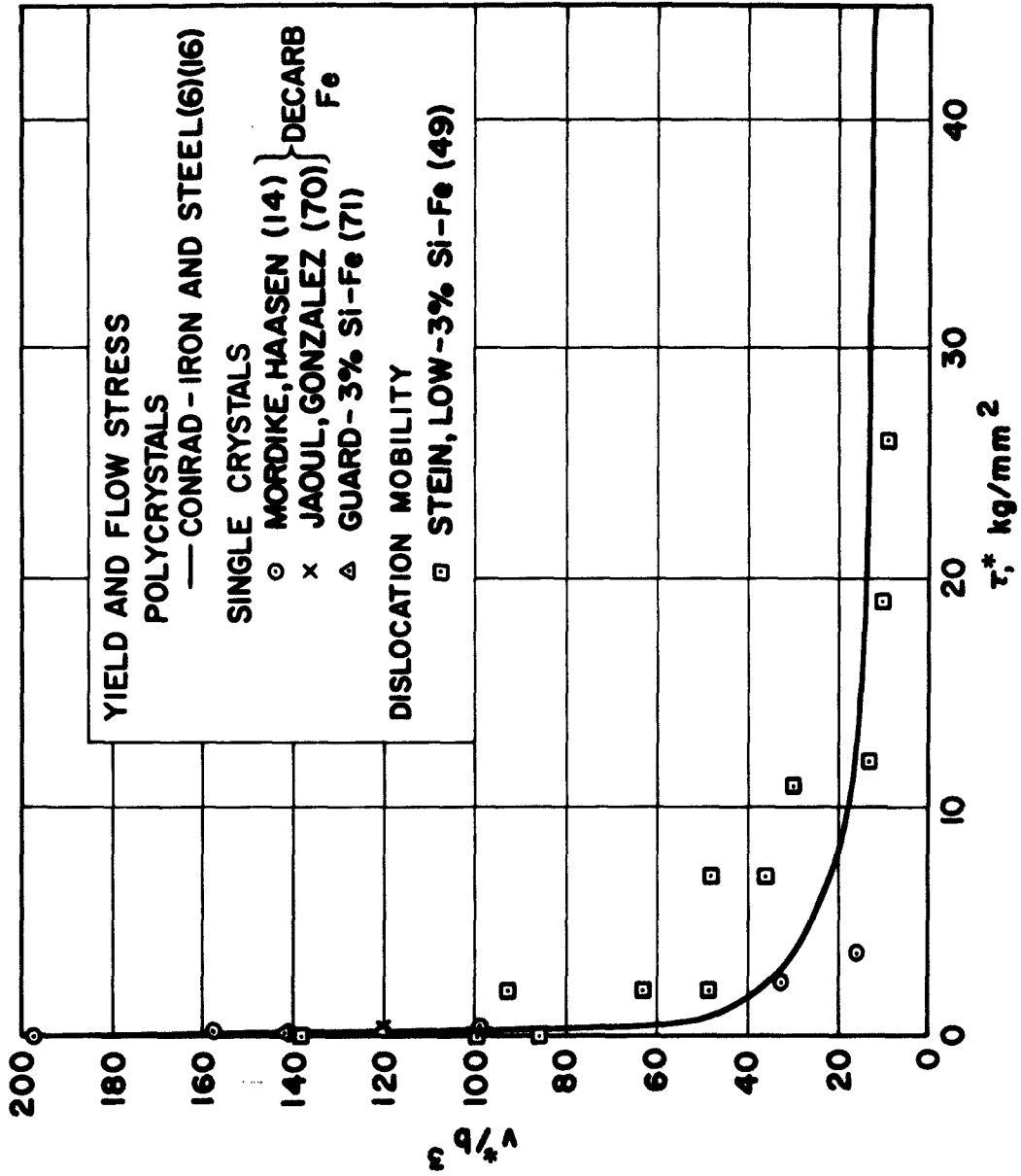


Fig. 23. Effect of Stress on the Activation Volume for Yielding and Flow in Iron and Steel

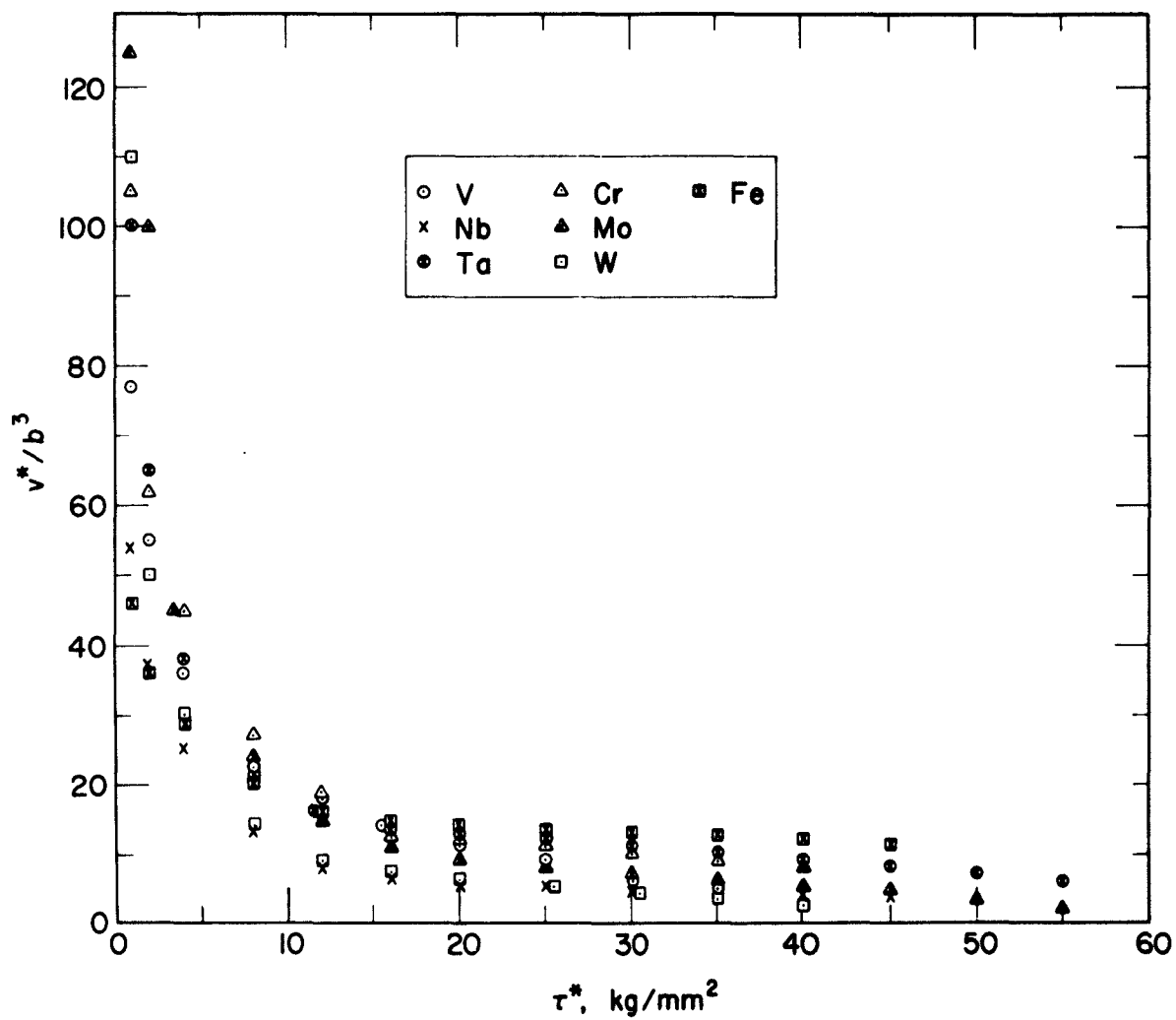


Fig. 24. Effect of Stress on the Activation Volume for Deformation of the B. C. C. Transition Metals

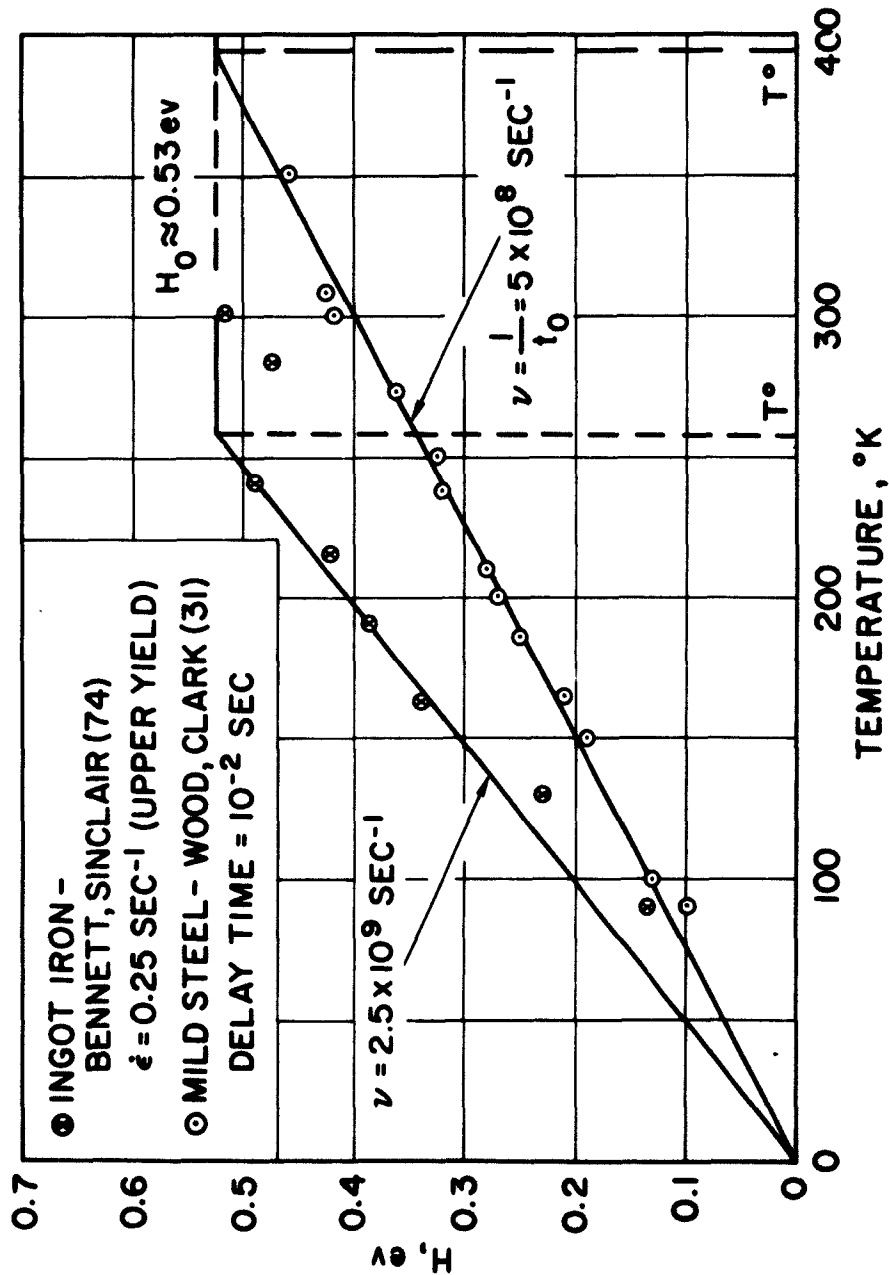


Fig. 25. Variation of Activation Energy with Temperature for Ingot Iron and Mild Steel

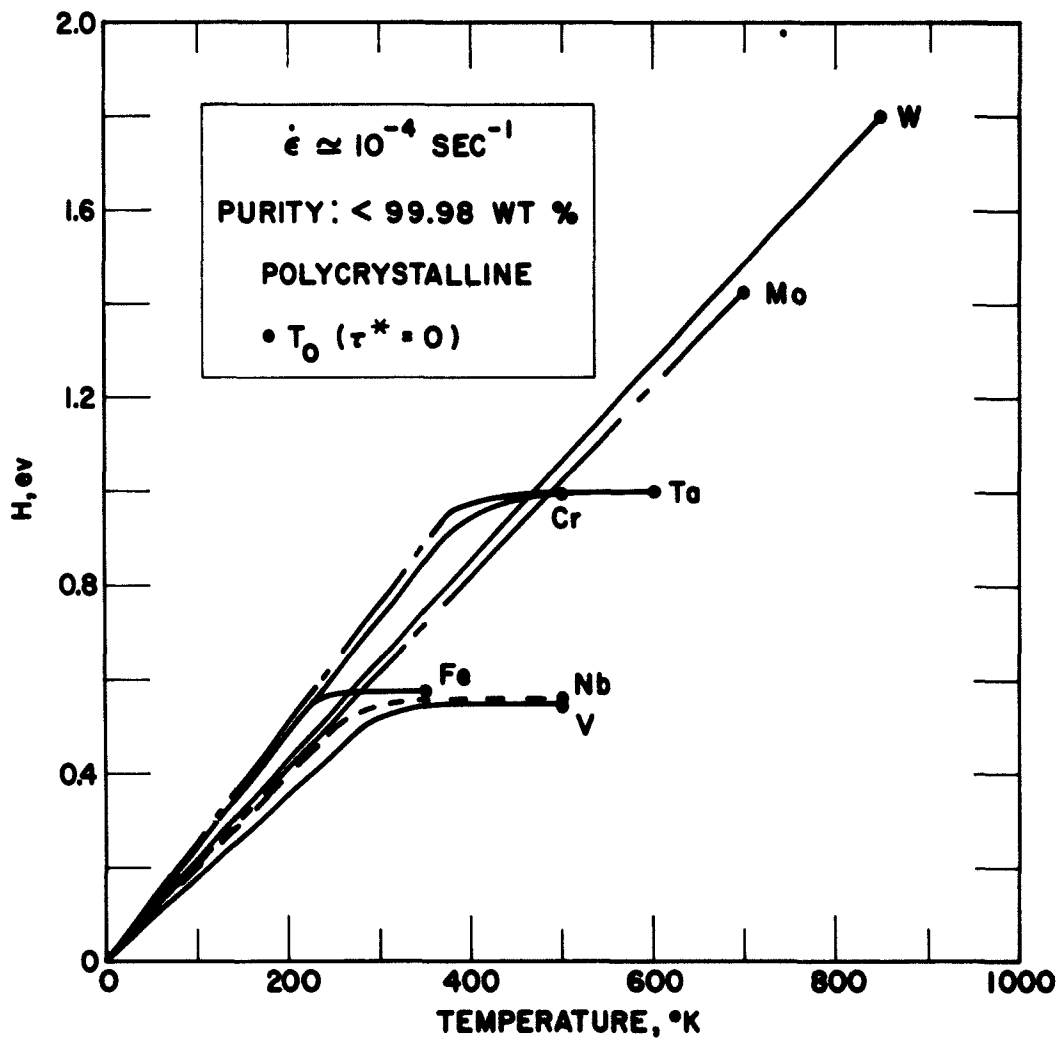


Fig. 26. Variation of Activation Energy with Temperature for Impure Polycrystalline B. C. C. Metals

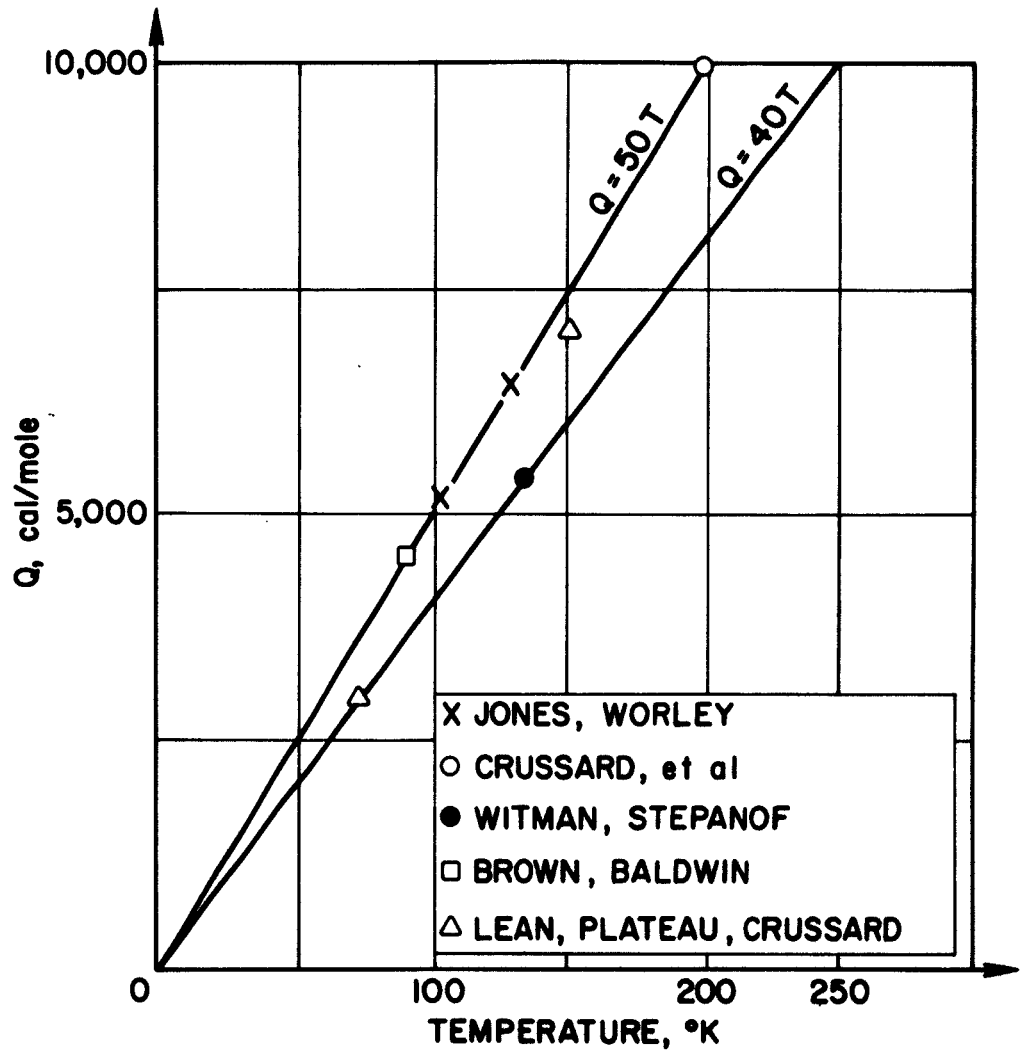
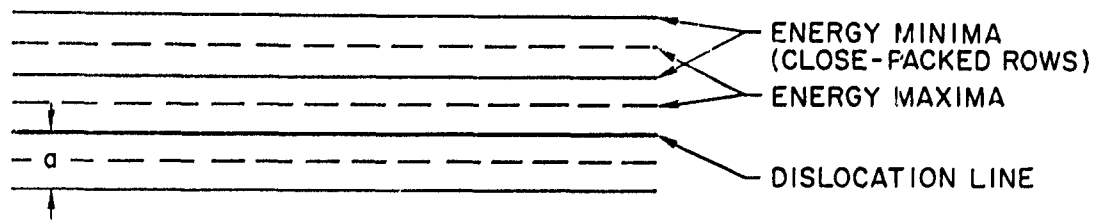
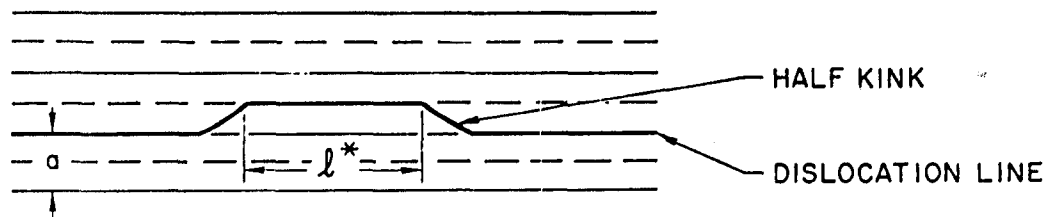


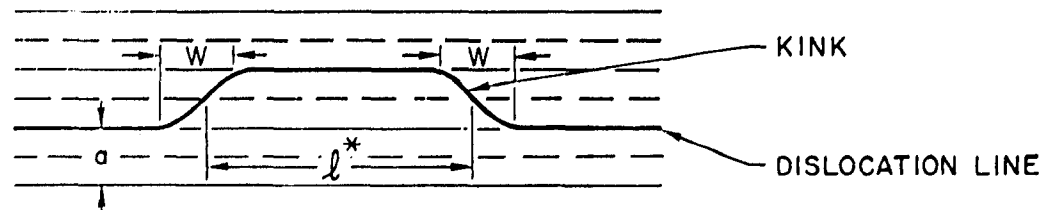
Fig. 27. Variation of the Activation Energy for Brittle Fracture with Temperature (from Lean et al., Ref. 38)



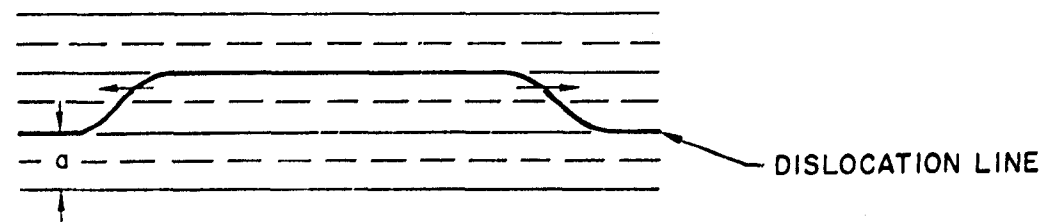
a. DISLOCATION LYING IN A CLOSE-PACKED DIRECTION.



b. INTERMEDIATE STAGE IN THE FORMATION OF A PAIR OF KINKS OF OPPOSITE SIGN.



c. FINAL STAGE IN THE FORMATION OF A PAIR OF KINKS.



d. LATERAL MOTION OF THE KINKS UNDER THE APPLIED STRESS.

Fig. 28. Seeger's Model for Thermally-Activated Overcoming of the Peierls-Nabarro Energy

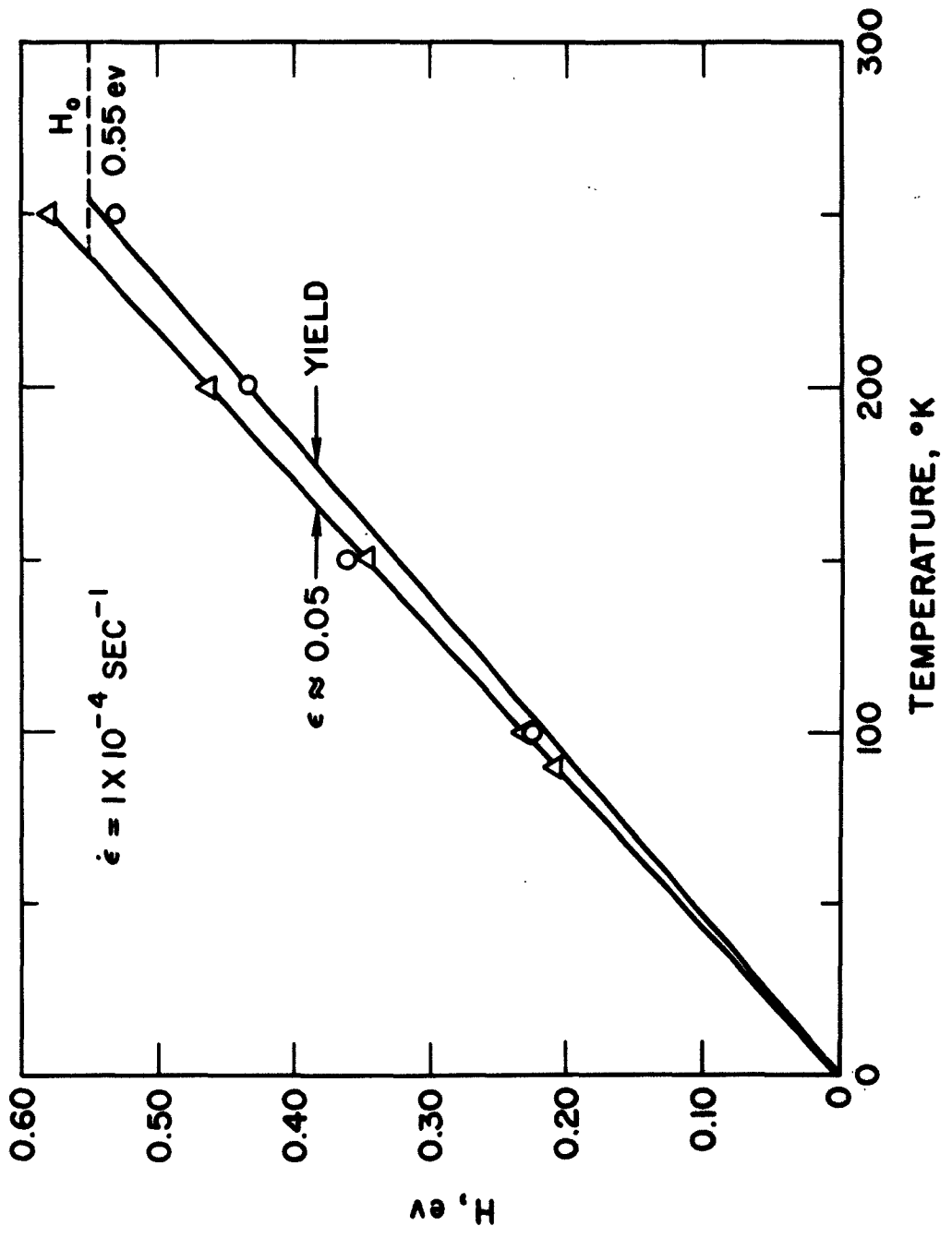


Fig. 29. Variation of Activation Energy with Temperature for Electrolytic Iron, Water Quenched from 920°C

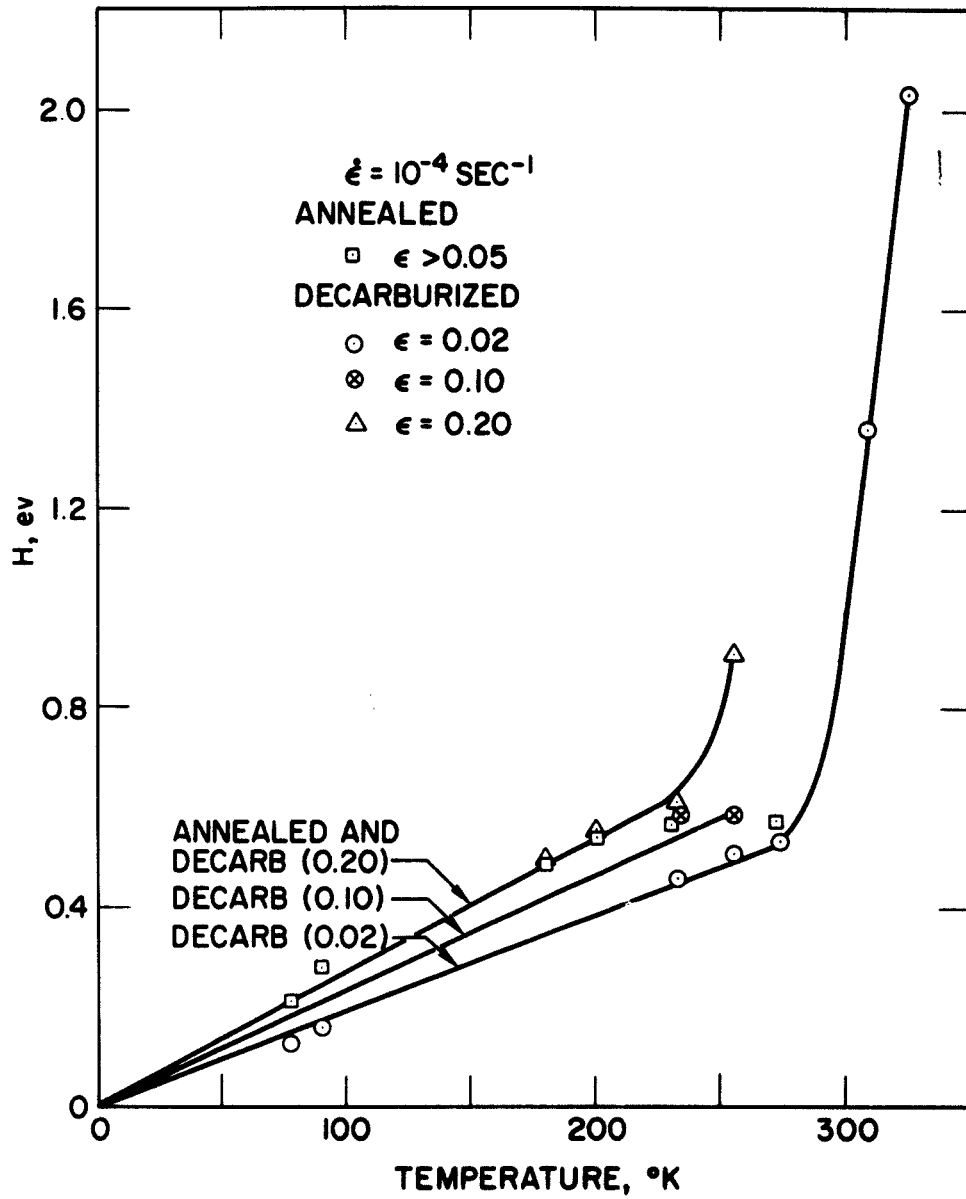


Fig. 30. Variation of Activation Energy with Temperature for Ferrovac Iron

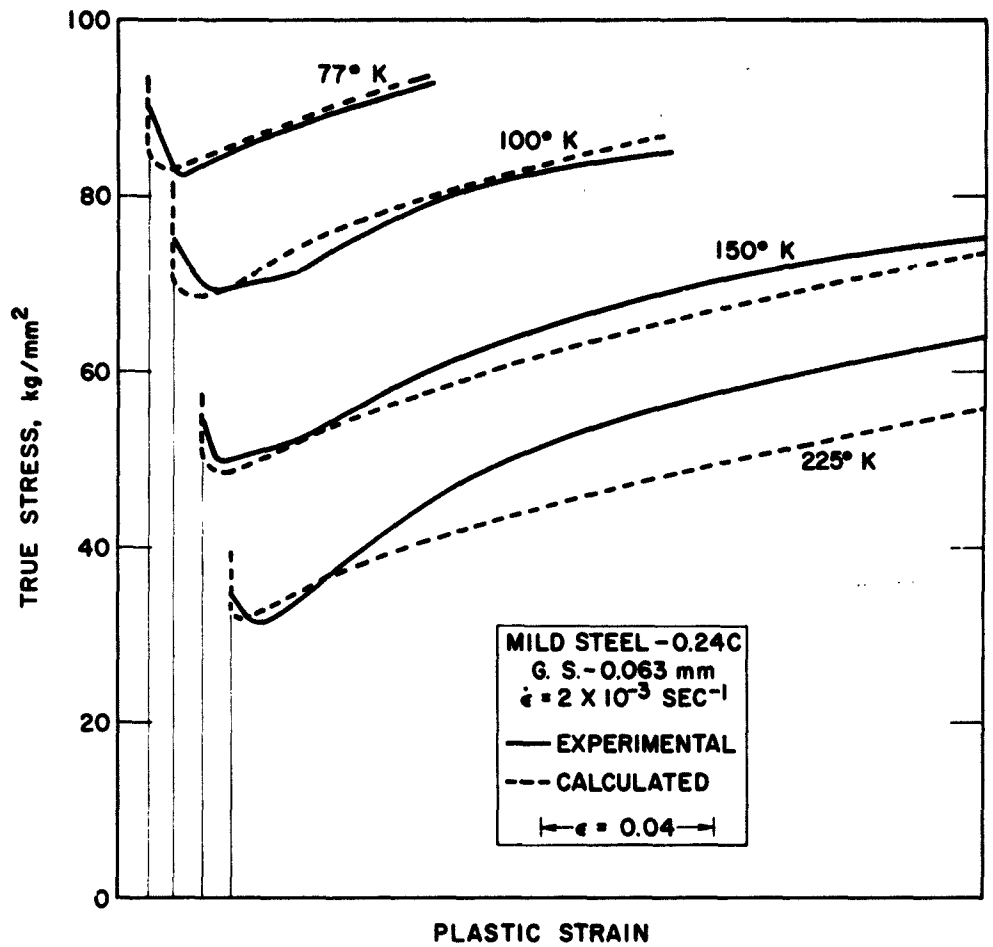


Fig. 31. Comparison of Calculated and Experimental Stress-Strain Curves for Mild Steel

REFERENCES

1. A. H. Cottrell, Rept. on the Strength of Solids, Phys. Soc., London, p. 30 (1948); paper presented at Conf. on High Rates of Strain, Inst. Mech. Eng. London, p. 448 (1957); Trans. AIME 212, 192 (1958).
2. A. H. Cottrell and B. A. Bilby, Proc. Phys. Soc. 62A, 49 (1949).
3. J. C. Fisher, Trans. ASM 47, 451 (1955).
4. N. F. Louat, Proc. Phys. Soc. B69, 454 (1956); Proc. Phys. Soc. B71, 444 (1958).
5. Z. S. Basinski and J. W. Christian, Australian J. Phys. 13, 299 (1960).
6. H. Conrad, J. Iron and Steel Inst. 198, 364 (1961).
7. J. W. Christian and B. C. Masters, "Thermally-Activated Flow in Body-Centered Cubic Metals," Res. Contract 7, Exptl, 729 (Nov. 1961).
8. H. Conrad and S. Frederick, Acta Met. 10, 1013 (1962).
9. H. Conrad and W. Hayes, "Correlation of the Thermal Component of the Yield Stress of the Body Centered Cubic Metals," TDR-169(3240-11)TN-3. Aerospace Corporation, El Segundo, California (1 March 1963); also "Thermally Activated Deformation of the B. C. C. Metals at Low Temperatures," to be published in Trans. ASM (March - June 1963).
10. J. Heslop and N. J. Petch, Phil. Mag. 1, 866 (1956).
11. G. Schoeck, Acta Met. 9, 382 (1961).
12. R. M. Rose, D. P. Ferris, and J. Wulff, Trans. AIME 224, 981 (1962).
13. B. L. Mordike, Z. Metallk. 53, 586 (1962).
14. B. L. Mordike and P. Haasen, Phil. Mag. 7, 459 (1962).
15. N. Brown and R. A. Ekvall, Acta Met. 10, 1101 (1962).
16. H. Conrad, "Yielding and Flow of Iron," TDR-169(3240-11)TN-3. Aerospace Corporation, El Segundo, California (27 February 1963); also to be published in High Purity Iron and Its Dilute Solid Solutions (AIME/J. Wiley and Sons, Inc., 1963).
17. G. A. Sargent and A. A. Johnson, "The Effects of Strain Rate and Temperature on the Plastic Deformation of Niobium," Fall Meeting AIME, New York (Oct. 1962).

REFERENCES (Continued)

18. P. J. Sherwood, "The Effect of Strain Rate on the Tensile Properties of Polycrystalline Tantalum at Room Temperature."
19. H. Schadler and J. R. Low, "Low-Temperature Brittleness of Refractory Metals," Contract No. Nonr-2614(00) (Apr. 1962).
20. H. Conrad, Phil. Mag. 5, 745 (1960).
21. H. Conrad and G. Schoeck, Acta Met. 8, 791 (1960).
22. K. Kitajima, Rept. presented to Res. Inst. of Appl. Mech. (Kyushu University, Japan), No. 15, 171 (1960).
23. F. de Kazinski, W. A. Backofen, and B. Kapadia, "Discussion of Ductile-Cleavage-Transition in Alpha-Iron," Fracture: Proc. International Conference on the Atomic Mechanisms of Fracture, B. L. Averbach, et al., ed. (John Wiley and Sons, Inc., New York, 1959), p. 65.
24. N. J. Petch, "Ductile-Cleavage-Transition in Alpha-Iron," Fracture: Proc. International Conference on the Atomic Mechanisms of Fracture, B. L. Averbach, et al., ed. (John Wiley and Sons, Inc., New York, 1959), p. 54.
25. W. Owen, paper presented at AIME Refractory Metals Symposium, Chicago (April 1962).
26. D. V. Wilson and B. Russel, Acta Met. 8, 36 (1960).
27. E. O. Hall, Proc. Phys. Soc. B64, 747 (1951).
28. N. J. Petch, J. Iron Steel Inst. 174, 25 (1953).
29. H. Conrad and B. Christ, "Variation of Dislocation Density and Stored Energy with Grain Size," TDR-169(3240-11)TN-6. Aerospace Corporation, El Segundo, Calif. (13 March 1963); also, to be published in Recovery and Recrystallization (AIME/Interscience Publishers, Inc.). H. Conrad, "Effect of Grain Size on the Lower Yield and Flow Stress of Iron and Steel," Acta Met. 11 (1), 75-77 (1963).
30. T. Tietz and J. Wilson, "Mechanical, Oxidation, and Thermal Property Data for Seven Refractory Metals and Their Alloys," Code 2-36-61-1. Lockheed Aircraft Corp., Missiles and Space Division, Sunnyvale, Calif. (Sept. 15, 1961).
31. D. S. Clark and D. S. Wood, Proc. ASTM 49, 717 (1949); Trans. ASM 43, 571 (1951); Trans. ASM 44, 726 (1952); Trans. ASM 46, 34 (1954).

REFERENCES (Continued)

32. J.M. Draft and A.M. Sullivan, Trans. ASM 51, 643 (1959).
33. H. Conrad and H. Wiedersich, Acta Met. 8, 128 (1960).
34. C. Zener and J.H. Hollomon, J. Appl. Phys. 15, 22 (1944).
35. T. Yokobori, Phys. Rev. 88, 1423 (1952).
36. J.D. Campbell, Acta Met. 1, 706 (1953); Trans. ASM 51, 659 (1959).
37. A.W. Magnusson and W.M. Baldwin, J. Mech. Phys. Solids 5, 172 (1957).
38. J.B. Lean, J. Plateau, and C. Crussard, Mem. Sci. Revise Metall. 56, 427 (1959).
39. R. Chambers, Paper presented at Fall Meeting AIME, New York (Oct. 1962).
40. A.H. Cottrell, Trans. AIME 212, 192 (1958).
41. J.R. Low and R.W. Guard, Acta Met. 7, 171 (1959).
42. A. Keh and S. Weissmann, paper presented at Conference on the Impact of Transmission Electron Microscopy on Theories of the Strength of Crystals, Berkeley (1961); to be published by Interscience Publishers, Inc.
43. D.P. Gregory and G.H. Rowe, "Mechanism of Work Hardening in B.C.C. Metals," PWAC-375, ASD Rept. TRD-62-354, July 12, 1962.
44. A. Seeger, Phil. Mag. 1, 651 (1956).
45. A. Seeger, H. Donth, and F. Pfaff, Discussions Faraday Soc. 23, 19 (1957).
46. A.H. Cottrell, Dislocations and Plastic Flow in Crystals (Oxford University Press, New York, 1953), p. 62.
47. D. Kuhlmann-Wilsdorf, Phys. Rev. 120, 773 (1960).
48. R. Hobart and V. Celli, J. Appl. Phys. 33, 60 (1962).
49. D.F. Stein and J.R. Low, J. Appl. Phys. 31, 362 (1960).
50. W.C. Leslie, Acta Met. 9, 1004 (1961).

REFERENCES (Continued)

51. L. E. Van Torne and G. Thomas submitted to Acta Met.
52. A. Brailsford, Phys. Rev. 122, 778 (1961).
53. J.S. Koehler, Phys. Rev. 86, 52 (1952).
54. E. Orowan, "Dislocations in Metals," AIME, 103 (1954).
55. W.G. Johnson and J. J. Gilman, J. Appl. Phys. 30, 129 (1959);
J. Appl. Phys. 31, 632 (1960).
56. T.A. Trozera, O. D. Sherby, and J.E. Dorn, Trans. ASM 49,
173 (1957).
57. R. P. Carreker and W. R. Hibbard, Acta Met. 1, 654 (1953).
58. J.H. Bechtold and P.G. Shewmon, Trans. ASM 46, 397 (1954).
59. J.H. Bechtold, Trans. AIME 206, 142 (1956).
60. J.W. Pugh, Proc. ASTM 57, 906 (1957).
61. "Investigation of the Properties of Tungsten and Its Alloys," WADD
Tech.Rept.60-144, Metals Res. Labs, Union Carbide Co. (May 1960).
62. H.G. Sell, et al, "The Physical Metallurgy of Tungsten and Tungsten
Base Alloys," Contract No. AF 33(616)-6933, Proj. No. 735101
(Jan. 12, 1962).
63. E. S. Tankins and R. Maddin, Columbium Metallurgy (Interscience
Publishers, Inc., New York, 1961), p. 343.
64. E. T. Wessel, L. L. France, and R. T. Begley, Columbium Metallurgy
(Interscience Publishers, Inc., New York, 1961), p. 459.
65. M. A. Adams and A. Iannucci, "The Mechanical Properties of
Tantalum with Special Reference to the Ductile-Brittle Transition,"
ASD Tech. Rept. 61-203 (Apr. 1, 1961).
66. M. J. Marcinkowski and H. A. Lipsitt, Acta Met. 10, 95 (1962).
67. R. W. Armstrong, "The Plastic Flow of Molybdenum from -200°C
to +400°C by Compression Tests," Westinghouse Res. Rept.
60-8-01-01-R3 (Nov. 7, 1955).

REFERENCES (Continued)

68. J. A. Hendrickson, D. S. Wood, and D. S. Clark, Trans. ASM 48, 540 (1956).
69. D. Weinstein, G. M. Sinclair, and C. A. Wert, "The Strain Rate and Temperature Dependence of the Ductile-to-Brittle Transition in Molybdenum Subjected to Torsional Loading," University of Illinois, Theoretical and Applied Mechanics Rept. No. 156 (Dec. 1959).
70. B. Jaoul and D. Gonzalez, J. Mech. Phys. Solids 9, 16 (1961).
71. R. Guard, Acta Met. 9, 163 (1961).
72. J. H. Bechtold, Acta Met. 3, 249 (1955).
73. J. W. Pugh, Trans. ASM 48, 677 (1956).
74. P. E. Bennett and G. M. Sinclair, University of Illinois, Theoretical and Applied Mechanics, Rept. No. 157 (Dec. 1959).

UNCLASSIFIED

UNCLASSIFIED

UNCLASSIFIED

UNCLASSIFIED

UNCLASSIFIED

UNCLASSIFIED

UNCLASSIFIED

UNCLASSIFIED

UNCLASSIFIED

UNCLASSIFIED

UNCLASSIFIED

UNCLASSIFIED

Aerospace Corporation, El Segundo, California.
**YIELDING AND FLOW OF THE BODY CENTERED
 CUBIC METALS AT LOW TEMPERATURES.**
 Prepared by Hans Conrad. 7 March 1963.
 [70 p. incl. illus.
 (Report TDR-169(3240-11)TN-5); SSD-TDR-63-30
 (Contract AF 04(695)-169) Unclassified report

The available experimental data on the mechanical behavior of the body centered cubic (b.c.c.) transition metals at low temperatures (<0.25 T_m) are reviewed and analyzed to establish the rate-controlling mechanism responsible for the strong temperature and the strain-rate dependence of the yield and flow stresses. The activation energy, H, activation volume, v*, and frequency factor, v, were determined as a function of the thermal component of the stress, σ^* . It was found that H₀ ($\sigma^* = 1 \text{ kg/mm}^2 \approx 0.1 \text{ lb/in}^2$), where μ is the shear modulus and b the Burgers vector; $v^* \approx 50 \text{ b}^3$ at $\sigma^* = 2 \text{ kg/mm}^2$, increasing rapidly to values in excess of 100 b^3 at lower stresses and decreasing to $2-5 \text{ b}^3$ at high stresses ($50-60 \text{ kg/mm}^2$); and $v = 10^6 - 10^{12} \text{ sec}^{-1}$, the higher

(over)

Aerospace Corporation, El Segundo, California.
**YIELDING AND FLOW OF THE BODY CENTERED
 CUBIC METALS AT LOW TEMPERATURES.**
 Prepared by Hans Conrad. 7 March 1963.
 [70 p. incl. illus.
 (Report TDR-169(3240-11)TN-5); SSD-TDR-63-30.
 (Contract AF 04(695)-169) Unclassified report

The available experimental data on the mechanical behavior of the body centered cubic (b.c.c.) transition metals at low temperatures (<0.25 T_m) are reviewed and analyzed to establish the rate-controlling mechanism responsible for the strong temperature and the strain-rate dependence of the yield and flow stresses. The activation energy, H, activation volume, v*, and frequency factor, v, were determined as a function of the thermal component of the stress, σ^* . It was found that H₀ ($\sigma^* = 1 \text{ kg/mm}^2 \approx 0.1 \text{ lb/in}^2$), where μ is the shear modulus and b the Burgers vector; $v^* \approx 50 \text{ b}^3$ at $\sigma^* = 2 \text{ kg/mm}^2$, increasing rapidly to values in excess of 100 b^3 at lower stresses and decreasing to $2-5 \text{ b}^3$ at high stresses ($50-60 \text{ kg/mm}^2$); and $v = 10^6 - 10^{12} \text{ sec}^{-1}$, the higher

(over)

Aerospace Corporation, El Segundo, California.
**YIELDING AND FLOW OF THE BODY CENTERED
 CUBIC METALS AT LOW TEMPERATURES.**
 Prepared by Hans Conrad. 7 March 1963.
 [70 p. incl. illus.
 (Report TDR-169(3240-11)TN-5); SSD-TDR-63-30.
 (Contract AF 04(695)-169) Unclassified report

The available experimental data on the mechanical behavior of the body centered cubic (b.c.c.) transition metals at low temperatures (<0.25 T_m) are reviewed and analyzed to establish the rate-controlling mechanism responsible for the strong temperature and the strain-rate dependence of the yield and flow stresses. The activation energy, H, activation volume, v*, and frequency factor, v, were determined as a function of the thermal component of the stress, σ^* . It was found that H₀ ($\sigma^* = 1 \text{ kg/mm}^2 \approx 0.1 \text{ lb/in}^2$), where μ is the shear modulus and b the Burgers vector; $v^* \approx 50 \text{ b}^3$ at $\sigma^* = 2 \text{ kg/mm}^2$, increasing rapidly to values in excess of 100 b^3 at lower stresses and decreasing to $2-5 \text{ b}^3$ at high stresses ($50-60 \text{ kg/mm}^2$); and $v = 10^6 - 10^{12} \text{ sec}^{-1}$, the higher

(over)

Aerospace Corporation, El Segundo, California.
**YIELDING AND FLOW OF THE BODY CENTERED
 CUBIC METALS AT LOW TEMPERATURES.**
 Prepared by Hans Conrad. 7 March 1963.
 [70 p. incl. illus.
 (Report TDR-169(3240-11)TN-5); SSD-TDR-63-30.
 (Contract AF 04(695)-169) Unclassified report

The available experimental data on the mechanical behavior of the body centered cubic (b.c.c.) transition metals at low temperatures (<0.25 T_m) are reviewed and analyzed to establish the rate-controlling mechanism responsible for the strong temperature and the strain-rate dependence of the yield and flow stresses. The activation energy, H, activation volume, v*, and frequency factor, v, were determined as a function of the thermal component of the stress, σ^* . It was found that H₀ ($\sigma^* = 1 \text{ kg/mm}^2 \approx 0.1 \text{ lb/in}^2$), where μ is the shear modulus and b the Burgers vector; $v^* \approx 50 \text{ b}^3$ at $\sigma^* = 2 \text{ kg/mm}^2$, increasing rapidly to values in excess of 100 b^3 at lower stresses and decreasing to $2-5 \text{ b}^3$ at high stresses ($50-60 \text{ kg/mm}^2$); and $v = 10^6 - 10^{12} \text{ sec}^{-1}$, the higher

(over)

UNCLASSIFIED

values of v generally being associated with the purer materials. H and v^* , as a function of stress, were independent of structure. This along with other observations indicates that the thermally-activated overcoming of the Peierls-Nabarro stress is the rate-controlling mechanism. The values of H_0 and the change in H with stress at low stresses are in agreement with those predicted by Seeger's model for the nucleation of kinks. The Peierls-Nabarro stress and kink energy derived from the experimental data are approximately $10^{-2}\mu$ and $4 \times 10^{-2}\mu b^3$, respectively. The experimental data suggest that the yield point in the b.c.c. metals is associated with the sudden multiplication of dislocations by the double cross-slip mechanism, which in turn is controlled by the motion of dislocations through the lattice. Stress-strain curves for mild steel calculated on the basis of this mechanism are in good agreement with the experimental curves.

UNCLASSIFIED

UNCLASSIFIED

values of v generally being associated with the purer materials. H and v^* , as a function of stress, were independent of structure. This along with other observations indicates that the thermally-activated overcoming of the Peierls-Nabarro stress is the rate-controlling mechanism. The values of H_0 and the change in H with stress at low stresses are in agreement with those predicted by Seeger's model for the nucleation of kinks. The Peierls-Nabarro stress and kink energy derived from the experimental data are approximately $10^{-2}\mu$ and $4 \times 10^{-2}\mu b^3$, respectively. The experimental data suggest that the yield point in the b.c.c. metals is associated with the sudden multiplication of dislocations by the double cross-slip mechanism, which in turn is controlled by the motion of dislocations through the lattice. Stress-strain curves for mild steel calculated on the basis of this mechanism are in good agreement with the experimental curves.

UNCLASSIFIED

UNCLASSIFIED

values of v generally being associated with the purer materials. H and v^* , as a function of stress, were independent of structure. This along with other observations indicates that the thermally-activated overcoming of the Peierls-Nabarro stress is the rate-controlling mechanism. The values of H_0 and the change in H with stress at low stresses are in agreement with those predicted by Seeger's model for the nucleation of kinks. The Peierls-Nabarro stress and kink energy derived from the experimental data are approximately $10^{-2}\mu$ and $4 \times 10^{-2}\mu b^3$, respectively. The experimental data suggest that the yield point in the b.c.c. metals is associated with the sudden multiplication of dislocations by the double cross-slip mechanism, which in turn is controlled by the motion of dislocations through the lattice. Stress-strain curves for mild steel calculated on the basis of this mechanism are in good agreement with the experimental curves.

UNCLASSIFIED

UNCLASSIFIED

values of v generally being associated with the purer materials. H and v^* , as a function of stress, were independent of structure. This along with other observations indicates that the thermally-activated overcoming of the Peierls-Nabarro stress is the rate-controlling mechanism. The values of H_0 and the change in H with stress at low stresses are in agreement with those predicted by Seeger's model for the nucleation of kinks. The Peierls-Nabarro stress and kink energy derived from the experimental data are approximately $10^{-2}\mu$ and $4 \times 10^{-2}\mu b^3$, respectively. The experimental data suggest that the yield point in the b.c.c. metals is associated with the sudden multiplication of dislocations by the double cross-slip mechanism, which in turn is controlled by the motion of dislocations through the lattice. Stress-strain curves for mild steel calculated on the basis of this mechanism are in good agreement with the experimental curves.

UNCLASSIFIED